THE UNIVERSITY OF ALBERTA

ZEEMAN EFFECT INVESTIGATIONS IN SINGLY IONIZED GADOLINIUM

by

DOLLARD DESMARAIS

A THESIS

SUBMITTED TO THE FACULTY OF GRADUATE STUDIES

IN PARTIAL FULFILMENT OF THE REQUIREMENTS FOR THE DEGREE

OF MASTER OF SCIENCE

DEPARTMENT OF PHYSICS

EDMONTON, ALBERTA

APRIL, 1967

UNIVERSITY OF ALBERTA

FACULTY OF GRADUATE STUDIES

The undersigned certify that they have read, and recommend to the Faculty of Graduate Studies for acceptance, a thesis entitled ZEEMAN EFFECT INVESTIGATIONS IN SINGLY IONIZED GADOLINIUM, submitted by Dollard Desmarais in partial fulfilment of the requirements for the degree of Master of Science.

ABSTRACT

A Zeeman effect investigation of singly ionized gadolinium has been attempted using a 7500 l.p.i. grating blazed for high orders in conjunction with a predispersive element. One hundred and twenty Zeeman patterns of the Gd II spectrum have been measured, from which g-values for 67 levels were calculated. Twenty-five of the better results are accurate to a mean error of 0.12%, whereas the overall accuracy is better than 0.5%.

This investigation has been made in order to verify the theoretical g-values as obtained by Smith and Wybourne. It has been found that their corrections from L-S coupling are in the right sense for 80% of the levels investigated, but agreement within experimental error was found for only 18% of the levels.

An attempt has been made to identify and determine the amount of mixing through configuration interaction in one heretofore unclassified level, the $4_{5/2}$ level. Finally, where observed g-values differed markedly from those predicted by Smith and Wybourne, a re-assignment of the energy levels involved was made, namely the levels of the multiplets $y\,^8P$ and $z\,^8F$, $z\,^8P$ and $z\,^{10}D$.

ACKNOWLEDGEMENTS

I would like to thank my advisor, Dr. E.H. Pinnington for initiating the project and for his encouragement and guidance throughout the past two years.

Special thanks are also due to Dr. S.B. Woods for the use of the magnet belonging to the Low Temperature Group.

I would also like to thank Mrs. Charlotte E. Moore-Sitterly for suggesting the choice of this element as a subject for research.

Finally I wish to thank the National Research Council for providing financial support for the duration of this work.

TABLE OF CONTENTS

LIST OF ILLUSTRATIONS

LIST OF TABLES

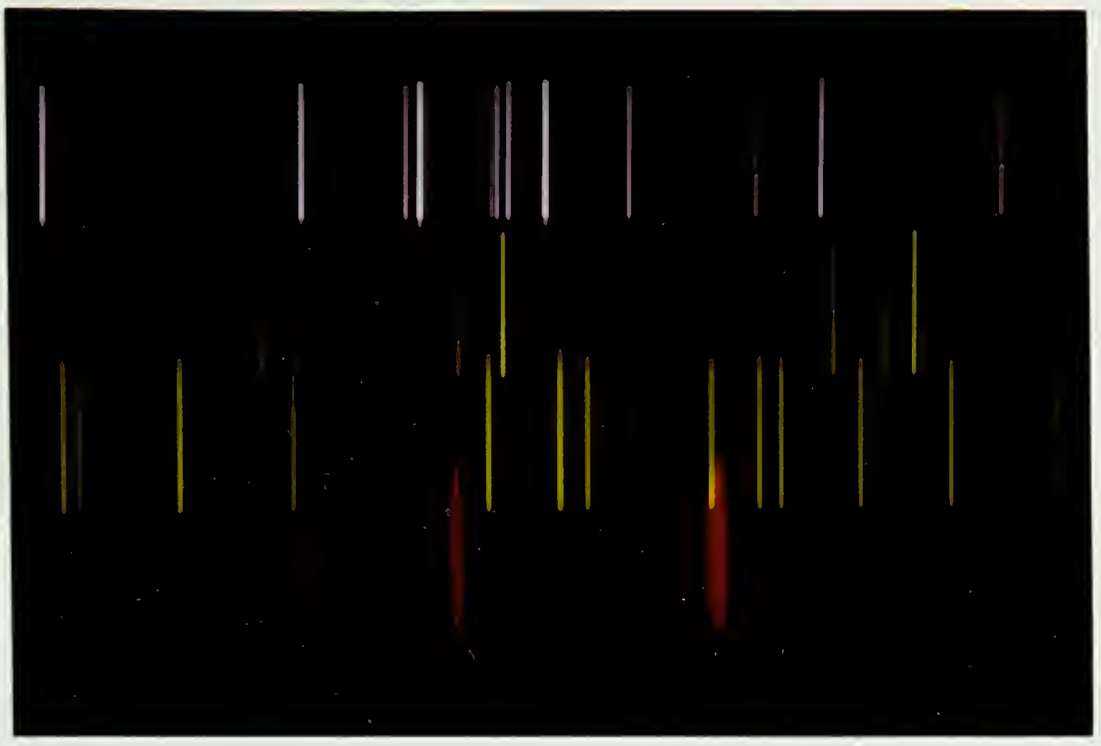

FIGURE 1.1

Section of

Typical Spectrogram

Obtained by Using High-Blaze Grating

in Conjunction with Predispersive Element

CHAPTER I

INTRODUCTION

The quantum states of an atom are in general modified when the atom is subjected to an external noncentral field. In particular, states which were formerly degenerate may be resolved, and certain spectral lines may consequently be split into several components. Such an effect caused by an electric field was discovered by Stark in 1913 and is known as the Stark effect (St 13).

A much more important case in spectroscopy is the so-called Zeeman effect, named after P. Zeeman who observed it in 1896 (Ze 97). However it may be questioned whether the priority for this discovery is properly his. Michelson (Mi 06) in his book "Light Waves and Their Uses" notes that Fievez recorded it a long time before. Zeeman announced only that the lines were broadened, whereas Fievez reported that each sodium line was doubled or quadrupled. In any case Zeeman probably made more immediate use of the discovery than Fievez. Faraday in 1812 had looked for the phenomenon but had used too low a resolving power.

On Lorentz's suggestion Zeeman sought and verified the existence of polarization at the edges of the broadened lines. After further improvement in technique the lines were resolved

into a triplet of polarized components. Lorentz was able to explain by his classical electromagnetic theory all the details of what eventually became known as the normal Zeeman effect.

Two years later Preston (Pr 98), making use of much higher resolution and dispersion, showed that most spectrum lines manifested more complex or "anomalous" patterns, which could not be explained by the classical theory. Runge correlated these results empirically with simple rational fractions of the normal triplet. The Landé splitting factor or g-factor was introduced by Landé (La 21) in 1921 to describe the anomalous Zeeman effect. The hypothesis of the spinning electron by Uhlenbeck and Goudsmit in 1925 (Uh 25) permitted calculation of these g-factors for energy states of known quantum character.

Zeeman effect studies were used extensively in the following years in the analysis of many spectra. The Zeeman effect at high magnetic resolution gives unique information regarding the total angular momentum of an electron as well as the Landé g-factors which are indicative of the orbital and spin quantum natures of these levels. A knowledge of the magnetic properties of the energy levels thus gained finds many uses today, e.g. in the interpretation of the solid-state magnetic properties of rare earth metals and compounds.

In recent years theoretical spectroscopists have attempted to further the knowledge of the more complex elements, particularly those of the rare earth category. These consist of two groups of fourteen elements each, known as the lanthanides and the actinides, depending on whether the 4f-shell or the 5f-shell is being filled. Pioneer among these is the "Racah Group" headed by G. Racah of the Hebrew University in Jerusalem. Zeeman studies have proven to be an important experimental check to the calculations of these theorists.

In 1965 G. Smith and B.G. Wybourne (Sm 65), then working at the Argonne National Laboratories, attempted an analysis of configuration interaction in the first stage of ionized gadolinium, Gd II*. The inclusion of both electrostatic and spin-orbit interactions as the major perturbations in the solution to the Schroedinger equation often yield energy levels which deviate by hundreds of wave numbers from the observed energy levels. It then becomes necessary to consider interactions not only within a configuration but with neighbouring configurations which are energetically close

---

* In atomic spectroscopy the stages of ionization are labelled by indicating the neutral (or un-ionized) atom, giving rise to the first spectrum, by the Roman numeral I and by increasing numerals for the successive stages of ionization giving rise to the corresponding successive spectra (Mo 58). Chemists usually assign Roman numerals according to the valence of the elements, so that Gd II would be written Gd (I) since it has lost one valence electron.

to the perturbed configuration. The eigenvectors resulting from the diagonalization of the energy matrices then express the states of the electrons in terms of linear combinations of the states of the connected configurations. For example a P term derived from the configuration $4f^7(^8S)6p6s$ was found by Smith and Wybourne to be mixed with D states derived from the $4f^7(^8S)5d6p$ configuration, and the $z\,^{10}D_{11/2}$ term was found to consist of the following mixture of terms: $31\%(^{10}D_{dp})$, $31\%(^{8}D'_{dp})$, $21\%(^{10}P_{ps})$. The g-values were calculated, but it was deplored that no reliable experimental values were available for comparison. "Zeeman data for some of the heavily mixed levels would provide an interesting test of our theoretical g_J values".(Sm 65)

The present project is an attempt to provide these experimentally measured g-values. The rare earth gadolinium has been found to be a particularly interesting element with which to work. Firstly the analysis of the spectrum is fairly complete. Some 5775 lines have been identified by A.S. King (Ki 43). Of these lines 1177 of Gd II and 1217 of Gd I have been classified by H.N. Russel (Ru 50). Hyperfine structure did not show up in any of the observed Zeeman patterns for the following reasons. The interaction between nuclear and electronic moments gives rise to the h.f.s. Now an atomic nucleus possesses a nuclear moment only if it has a nonzero nuclear spin. Gadolinium being of even atomic

number, all its isotopes of even atomic weight have zero nuclear spin. Thus 70% of naturally occuring Gd gives no h.f.s. The intensity of the h.f.s. components for the remaining 30% was so weakened that none was actually observed.

One hundred and twenty Zeeman patterns of the Gd II spectrum have been measured, from which g-values for 67 levels were calculated. An attempt has been made to determine the relative amount of configuration interaction occuring in an unclassified level, the $^4_{5/2}$ level. Where observed g-values differed markedly from those predicted by Smith and Wybourne, a re-assignment of the energy levels was made for a limited number of cases.

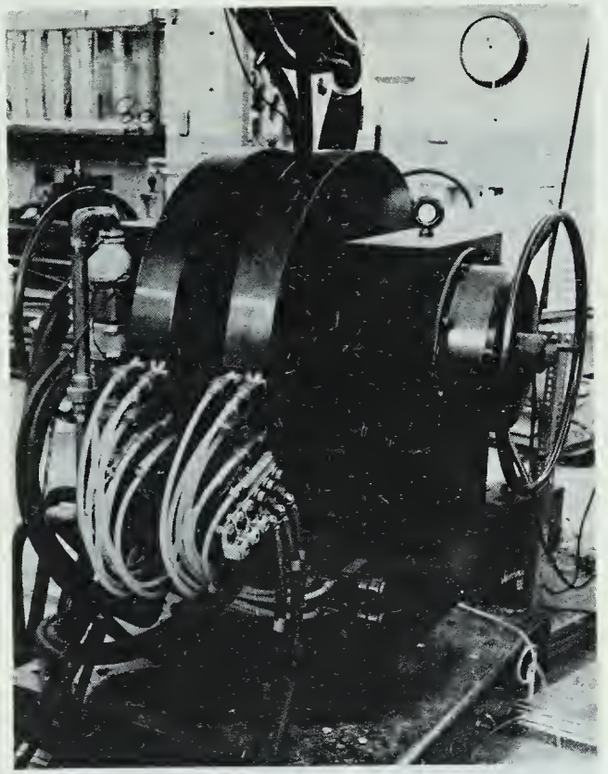

Fig. 1.2

Electromagnet

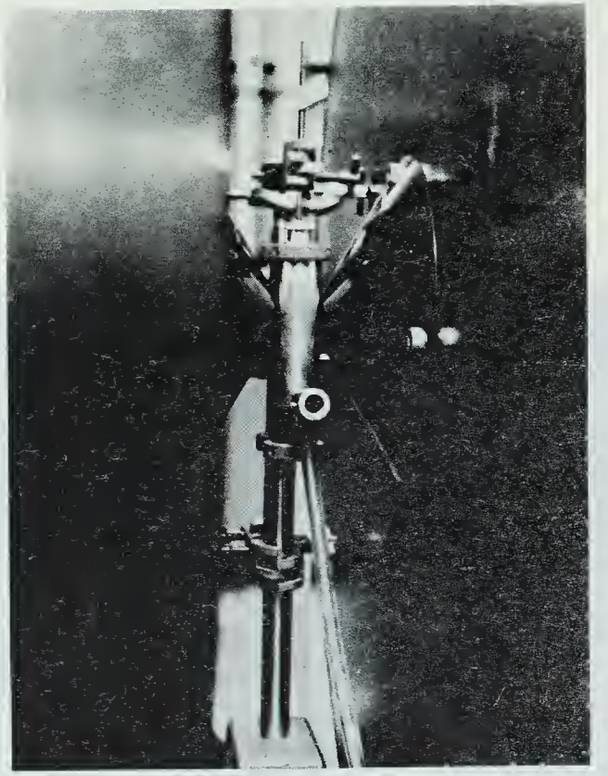

Fig. 1.3

Cavity in Magnet

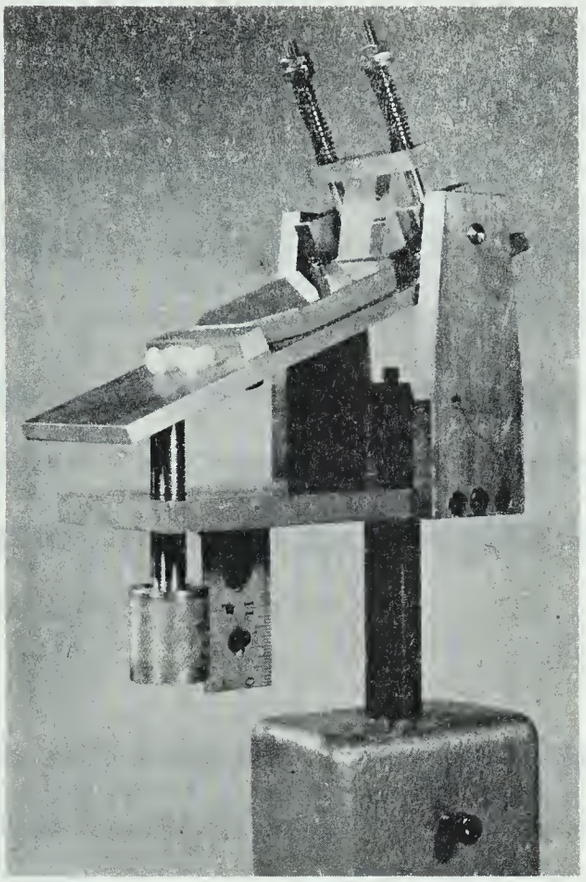

Fig. 1.4 Order Sorter

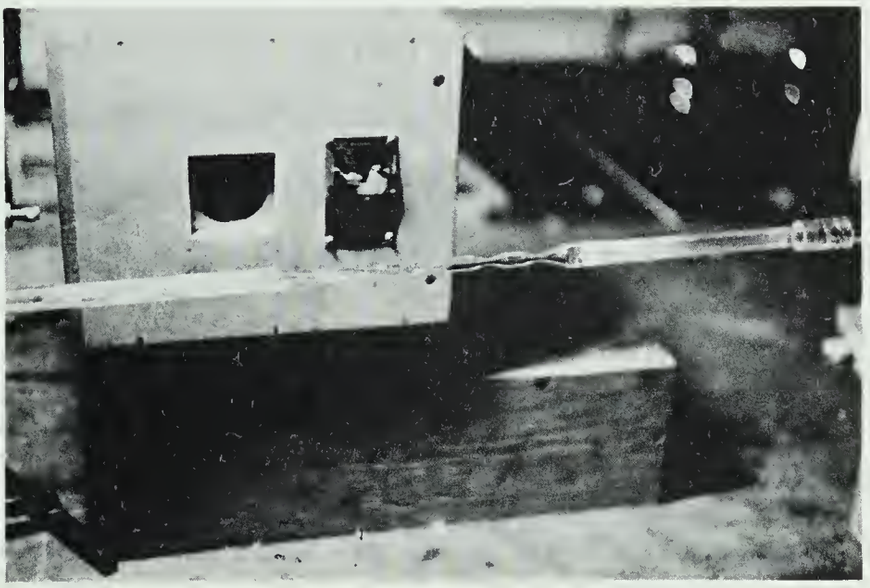

Fig. 1.5 Furnace & Receiving Tube

CHAPTER II

APPARATUS AND EXPERIMENTAL PROCEDURE

The apparatus used in this investigation of the Zeeman effect in Gd II consists generally of the following components: electrodeless discharge lamps with ancillary equipment, an electromagnet, a 3.4 meter Ebert spectrograph, an order sorter, a fairly simple optical system, and a spectrum plate comparator with photoelectric setting.

2.1 Microwave Generator, Electromagnet, Grating and Spectrograph

The electrodeless discharge lamps, to be discussed later under the heading Tube making, were excited by a Raytheon Model KV-104 Microwave Power Generator operating in the 2400-2500 megacycle band at 12.2 cm wavelength (2450 mc), and equipped with a tuneable air-cooled microwave cavity. Since the meter built into the generator read only the algebraic sum of the forward and reflected power, an additional meter was installed on the output which read both forward and reflected power. The best adjustment of the cavity was achieved at minimum reflected power and whatever forward power was desired. This meter may be obtained from Microwave Devices Co., Farmington, Conn., and has proved to be definitely superior to the built-in meter for obtaining proper resonance of the cavity.

The electromagnet (fig. 1.2, p. 7)was fitted with 1.25 in. diameter tapered pole caps. It was a model 12C-AT-LI from Pacific Electric Motor Co., Oakland, California. A field of about 30 kilogauss was obtainable for a power dissipation of 20 kw, the magnet being operated at 750 amperes. Because of their small diameter, the pole pieces were almost saturated at this power. The magnetic field obtained by running the magnet at full power (40 kw) was only approximately 8% higher than at 20 kw. The lower power was used to avoid over-heating the power supply. The coils were internally water cooled at 7.2 G.P.M., 60 psi pressure drop, with a maximum temperature rise of 40 C^{o}. The current was manually regulated to give a field stable to $\pm 0.1\%$. This magnet and its associated power supply were made available by the Low Temperature Group.

The 3.4 meter Ebert Spectrograph was used with a 7,500 l.p.i. grating blazed for the 9th to 20th orders in the range 6,000Å to 3,000Å. The linear reciprocal dispersion obtainable in the 10th order was 0.5 Å/mm. The use of a grating blazed for such high orders obviously required some method of sorting out the orders. For this purpose an order sorter was devised, the principle of which will now be discussed.

2.2 Order Sorter

Prior to the use of high angle blaze gratings in conjunction with predispersive elements, measurement of g-values by the usual methods of optical spectroscopy were seldom accurate to more than 1 in 200 (Wy 65). It will be seen from the discussion in chapter V that the accuracy for most g-values measured in the present programme is considerably better than 0.5%. This marked improvement in accuracy is due to the use of a grating blazed to such high orders coupled with a predispersive element which is both simple to construct and to operate.

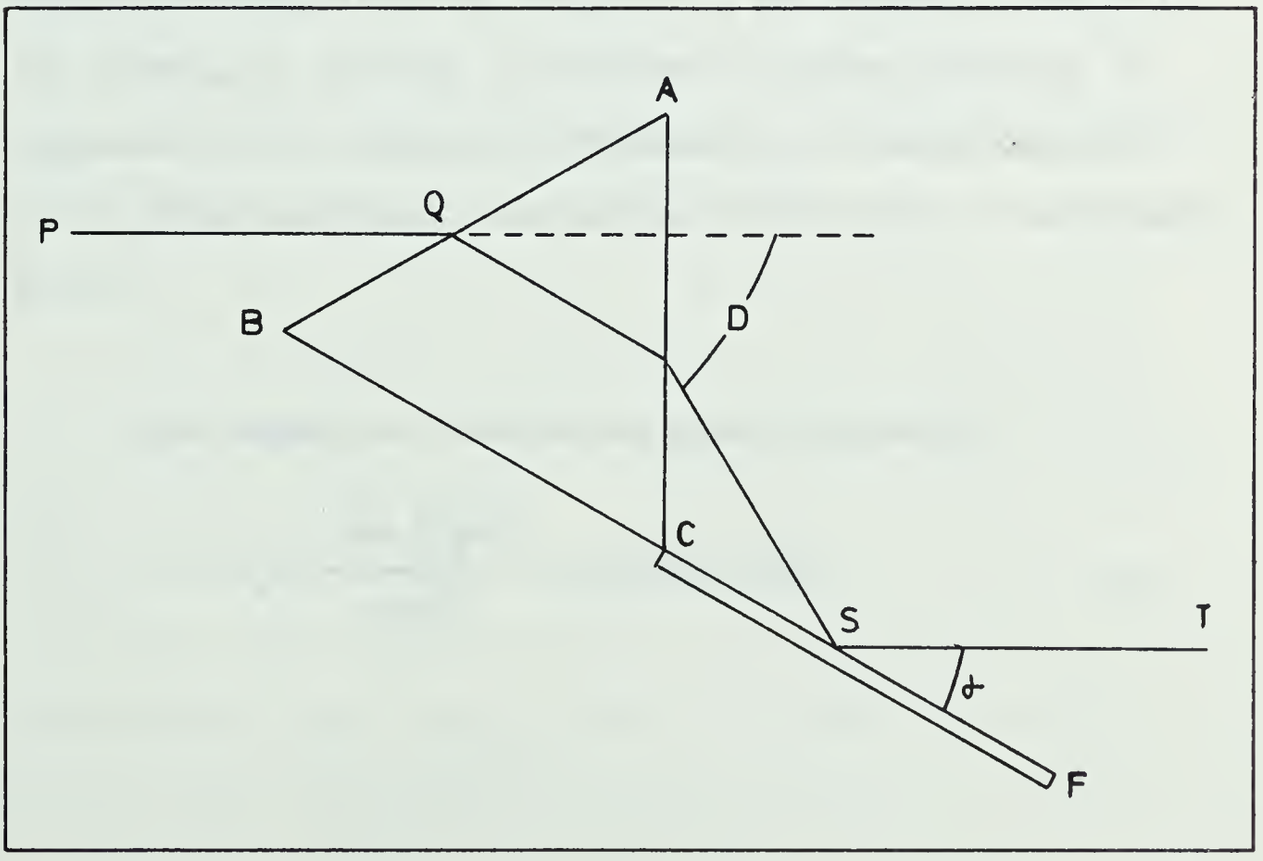

Figure 1.6

The order sorter used (fig. 1.6, p. 11) is essentially a Wadsworth prism-mirror arrangement (Sa 63). A monochromatic beam enters the prism at minimum deviation and emerges displaced but not deviated from its original direction. Such an arrangement has the distinct advantage over various earlier predispersive elements in that it may be placed directly on the optical bench of the spectrograph. In the type used by Davis at Berkely (Re 63), the beam is refracted horizontally and hence at an angle with the optical bench, which arrangement can be a disadvantage especially if space is at a premium.

In the figure (p. 11), ABC is a 60^{o} prism, CF a front-surface silvered mirror and the plane of the diagram is vertical. The incoming ray PQ which is refracted at minimum deviation, is displaced by the prism-mirror arrangement, but emerges parallel to PQ. Other wavelengths will give rays travelling at small angles to ST.

The refractive index of the prism is given by

$$n_{\lambda} = \frac{\sin \frac{A + D}{2}}{\sin \frac{A}{2}} = 2 \sin(30 + D/2) \qquad (1)$$

Since the deviation D is cancelled by reflection at the mirror, $\alpha = D/2$, where α is the angle that the plane of reflection makes with the horizontal. Hence

$$\alpha_\lambda = \sin^{-1}(n_\lambda/2) - 30 \qquad (2)$$

If the prism is so placed that light of wavelength λ strikes the center of the spectrograph slit, then light of wavelength $\lambda \pm \Delta\lambda$ will strike immediately below and above this point. If green falls at the center, then red will fall below and blue above. For each of these wavelength intervals, the grating equation $m\lambda = 2d\sin\theta$ will apply, with the result that the red, green and blue are diffracted by the grating into their respective spectra, each in its own order (fig. 1.1, p. 1).

In order to vary the order m which appears along the centre of the camera aperture, it is only necessary to vary α according to equation (2). The prism mount is so pivoted that the height of the beam is unaltered by rotation of the plane of reflection. The spatial separation of neighbouring orders on the photographic plate is given by $\frac{dD}{d\lambda}\Delta\lambda L$ where L is the distance from the prism to the entrance slit and $\Delta\lambda$ is the separation of two wavelengths in consecutive orders which would appear at the same position on the plate were the order sorter removed. For example, $\lambda = 2850\text{Å}$ in the 20th order would appear in the same position as $\lambda = 3000\text{Å}$ in

in the 19th order, so that $\Delta\lambda$ is 150Å. Now since light is passing through the prism either at or close to minimum deviation, it is possible to write

$$\frac{dD}{d\lambda} = \frac{dD}{dn}\frac{dn}{d\lambda} = \frac{2\sin\frac{A}{2}}{(1 - n^2\sin^2\frac{2A}{2})^{\frac{1}{2}}}\frac{dn}{d\lambda} = \frac{1}{(1 - n^2/4)^{\frac{1}{2}}}\frac{dn}{d\lambda} \qquad (3)$$

The value of $dn/d\lambda$ may be found from a plot of refractive index versus wavelength for the material used. At 3000Å for fused quartz, $\Delta\lambda$ for m = 19 to m = 20 is 150Å, and $dn/d\lambda = 4.7 \cdot 10^{-5}$ rad/Å, so that a separation of 2 mm of these two orders requires L to be 28 cm. Because of absorption at certain wavelengths and the way in which n varies with λ, it was found best to use three different prisms to cover the whole spectrum adequately: fused quartz in the ultraviolet, crown glass in the intermediate regions, and flint glass in the long wavelength region.

The order sorter here described has been found simple to use and reproducible in setting. It is also easy and inexpensive to construct, the most costly item being the 60° ultraviolet grade fused quartz prism.

2.3 Tube Making

The tube making procedure was essentially that discussed in the literature (Wo 63) and may be briefly summarized as follows. Quartz preparation tubes 6 mm in outside diameter and 12 cm long were first thoroughly cleaned with nitric acid and distilled water and heated in a furnace. About 20 mgm of 99.99% pure gadolinium was introduced into each tube, together with about 40 mgm of iodine. The tubes were then evacuated to about 10^{-3} mm mercury and sealed off into lengths of about 6 cm, with one end being pulled to a thread-like point. A set of about six such tubes were placed in a furnace and heated for about an hour. The tubes then turned to a rich brown color.

Quartz receiving tubes 8 mm in inside diameter and about 30 cm long were cleaned and five constrictions were made near the middle of each tube (fig. 1.5, p.8). These constrictions were to facilitate sealing off and separation of the receiving tubes to form four microwave tubes, each about 4 cm in length.

The receiving tube was attached by means of a short length of tygon tubing to the vacuum system consisting of a mercury diffusion pump and a backing pump. The tip was broken off a preparation tube which was then introduced into the receiving tube. The system was sealed with the preparation tube as far back from the constrictions

as possible. A furnace was placed around the section of the receiving tube which would eventually form the microwave tubes. This section was then degassed, keeping meanwhile the preparation tube cool by means of a dampened cloth. By gently tapping on the receiving tube the preparation tube was then advanced until its tip led into the microwave tubes. The furnace was placed around the preparation tube and the gadolinium iodide was distilled into the microwave tubes. This stage in the process proved to be critical. A white deposit, gadolinium iodide, was found to be formed on the walls of the microwave tubes. With further heating, either this deposit turned black, or else some black compound was distilled from the preparation tubes. It was found that the best results were obtained when heating was stopped before this blackening occured. The furnace was then removed, the microwave tubes sealed off from the section containing the preparation tube, and the pressure brought down to 10^{-5} mm mercury. The gadolinium iodide was distilled evenly over the four microwave tubes by means of a torch and each tube was then sealed off and attached to a quartz rod, to permit suspension inside the microwave cavity (fig. 1.3, p. 7).

Of the four microwave tubes prepared in this way, usually two or three would function quite well. The discharge was started normally by means of a high-frequency leak-tester. Some

tubes would start instantly, others would need ten to twenty minutes of alternate heating and cooling in liquid nitrogen. Once the discharge went out, the tube ordinarily could not be restarted immediately, but it was found that it would work again a day or so later. The type of quartz used in making the microwave tubes would also seem to be a factor in their succesful operation. After having made excellent tubes for some weeks, it suddenly became impossible to produce any that would work. The only possible explanation would seem to be that quartz from a different supplier had been used. Workers in the U.S. have noticed the same thing. For example, tubes made at Argonne would work at Berkely, whereas those made locally would not.

In all some 50 tubes were made, of which about 50% were eventually made to function with varying degrees of success. Tube manufacture was thus not too great a problem.

2.4 The Optical System

The electromagnet was situated in a neighbouring laboratory, across a corridor from the spectroscopy lab. (fig. 1.7, p. 18). Holes had to be made in the two walls separating the labs, so that light leaving the microwave cavity, and made parallel by a quartz achromat of focal length 10 in (lens #1), could reach a plane mirror located next to the optical bench, a distance of 36 ft.

FIG. 1.7
SCHEMATIC OF OPTICAL SYSTEM

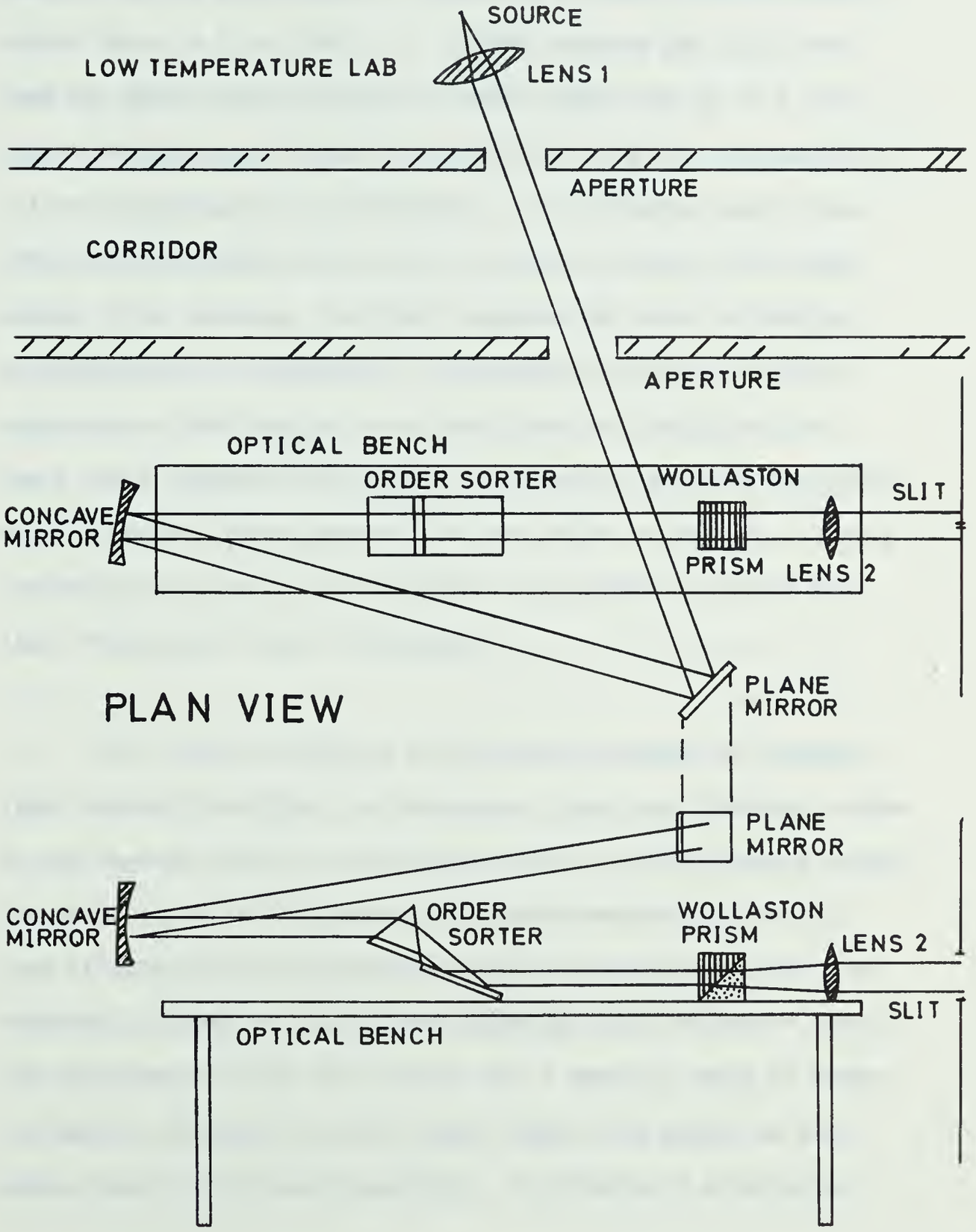

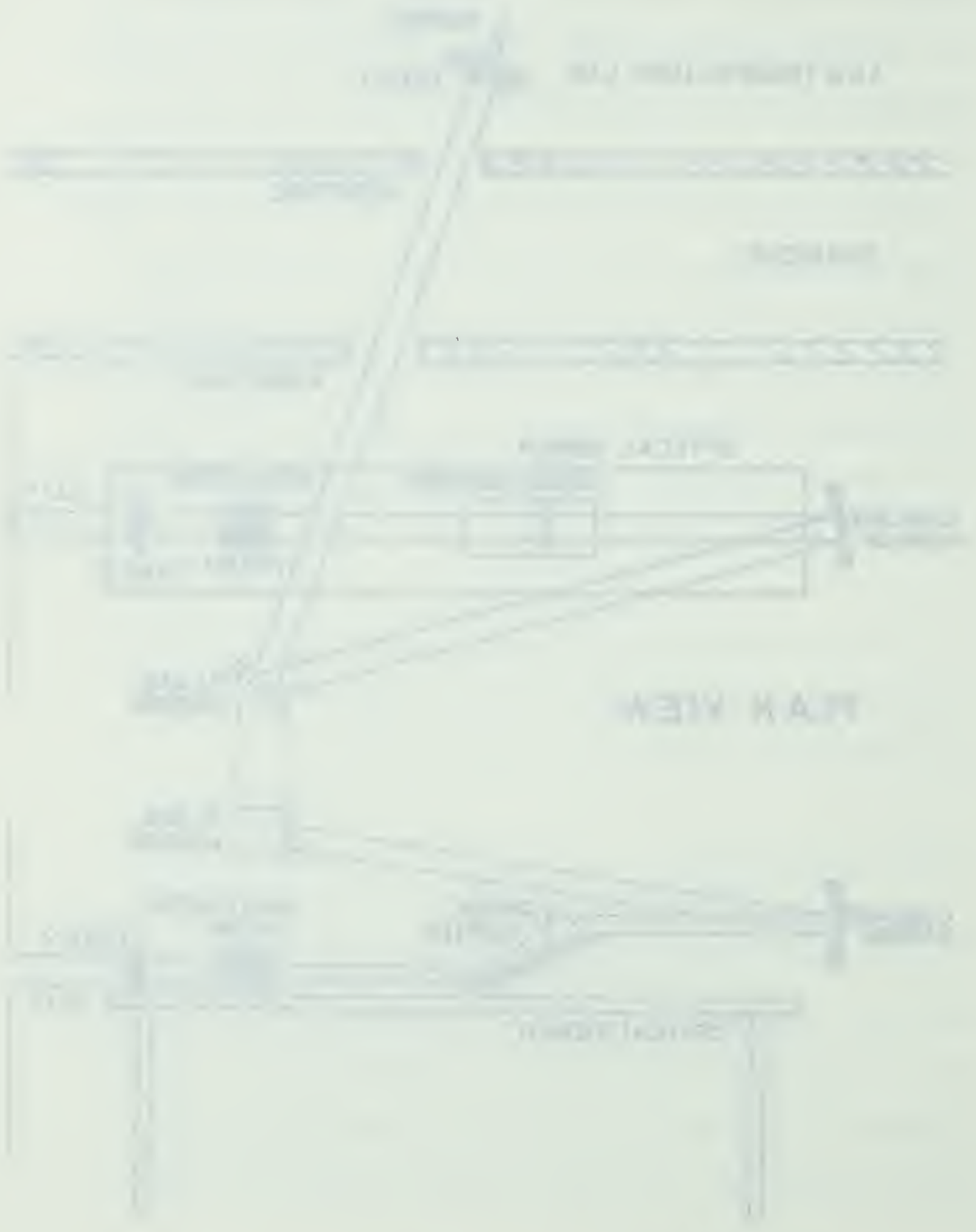

After reflection from the plane mirror, the light was focused on the slit of the spectrograph by means of a front-surfaced concave mirror (diam. 4.5 in, f=45 in). Before reaching the slit, the beam was made to pass through the order sorter and on to a 2 cm-square Wollaston prism which separated the beam into its parallel (π) and perpendicular (σ) components. An additional quartz lens (f=10 in) was placed at the slit in order to control the illumination of the grating. The Ebert spectrograph being stigmatic, no difficulty was encountered in bringing the various vertical components of the spectrum to a sharp focus on the plate, i.e. the π and σ components which were separated by the Wollaston prism and the various orders separated by the order sorter. By removing the Wollaston prism it was possible to photograph the field-free lines between the π and σ components.

The initial lining up of the mirror was done by placing a light source (flashlight) on the optical bench and directing a beam on the reverse path from the concave mirror to the microwave source, the order sorter and Wollaston prism being temporarily removed. Lens #1 could thus be adjusted so that the reversed beam would be accurately focused on the pin-hole opening in the microwave cavity. The adjustement of the order sorter for a specific range of orders was made by setting it so that green light would appear as the middle order in the camera aperture. By rotating a setscrew on

the instrument, it was then a simple matter to obtain the desired range of orders.

2.5 Photographic Plates and their Measurement

The spectrum of gadolinium was recorded using three spectrometer settings and a range of orders from the 9th to the 20th. Zeeman patterns were obtained at two exposure times, 5 min. and 20 min., with a zero-field spectrum of one minute being taken between the π and σ components. Kodak 103a-F plates were used in the 5000Å to 7000Å range and Ilford Zenith Astronomical plates below 5000Å. The latter are reputed to be faster for relatively long exposures (i.e. longer than 5 minutes).

The spectrum was identified using charts prepared by Gatterer and Junkes (Ga 59), with some known line of the mercury spectrum as a starting point. In order to photograph the region 2900Å to 6500Å, it was only necessary to use three reproducible settings of the grating. The dispersion as a function of distance along the plate was measured for each of these settings. This information was then plotted on a graph, which could be read to an accuracy which was within experimental error.

The Zeeman patterns were measured on a spectrogram comparator with photoelectric setting (To 51). To avoid any personal

errors, all patterns were measured twice, once with the plate moving from left to right on the comparator and once right to left. The separations in microns of the Zeeman components in each pattern were converted into Å-units using the dispersion graph. These intervals were then converted into energy units (cm^{-1}) using Kayser's Tabellen der Schwingungszahlen (Ka 25) which include a correction from the wavelength in air to that in vacuum. Measurements of the patterns were found to be reproducible to ±1 micron on the plate, which corresponded to an uncertainty of about ±0.002 cm^{-1} in the pattern itself. In those cases where complicated Zeeman patterns obviously overlapped, the components of each pattern were first identified by searching for components of equal spacing using a photographic enlarger.

2.6 Determination of Magnetic Field Strength

The Zeeman splitting being proportional to the magnetic field, the latter must be known within experimental error to calculate g-values from the observed pattern. As mentioned previously (p. 10) the magnetic field was stable to ±0.1% during a definite exposure; however it was found not reproducible to this accuracy in subsequent exposures. This was probably not due to the magnet, but rather to the fact that the microwave tube could never be placed in exactly the same position in the cavity. By testing this field with a rotating coil gaussmeter, there was found to be

considerable variation in the field for a displacement of the tube by a few millimeters. Efficient operation of the microwave tubes proved to be very sensitive to the positioning of the tubes in the magnetic field. The position giving maximum intensity varied from tube to tube, and sometimes from exposure to exposure for the same tube. Since maximum intensity was the major criterion, it was not possible to guarantee that each tube was operated exactly at the position of maximum magnetic field strength. It was impossible therefore to be certain of the field for a given exposure.

Thus the field for each exposure had to be calibrated from the Zeeman patterns themselves. This problem was quite a crisis in the present work. Fortunately g-values had been calculated for certain low-lying energy levels of neutral gadolinium by atomic beam methods. The following values are due to Smith & Spalding (Sm 61).

Level	g-Value
$a\,^9D^o_6$	1.67 ±.02
$a\,^9D^o_5$	1.73 ±.01
$a\,^9D^o_4$	1.8392 ±.0005
$a\,^9D^o_3$	2.0708 ±.0004
$a\,^9D^o_2$	2.6514 ±.0006

The actual field for each exposure was determined in the following way. The field strength was initially determined by photographing the spectrum of neon using a quartz tube containing neon at a pressure of about 1 mm Hg. The neon spectrum was photographed immediately following the Zeeman photograph of gadolinium without switching the magnet off between the gadolinium and neon exposures. Exact g-values of neon having recently been calculated in this laboratory (Pi 67), it was possible to determine the field corresponding to a given position of the neon tubes to a high accuracy. In fact, the neon tubes being much easier to excite, it was always possible to guarantee that they were operated at the position of maximum field strength, the value of the field obtained from the neon patterns agreeing with that measured using a rotating coil gaussmeter to within 0.1%, the specified accuracy of the gaussmeter.

Zeeman patterns for gadolinium lines involving those energy levels for which g-values had been calculated by atomic beam methods were measured and their corresponding g-values calculated using the field as obtained from the neon patterns. These were found to be in the same ratio to each other as the corresponding ratios of the g-values obtained by atomic beam methods, but differed from the latter by a constant factor. This variation was due to the neon-measured field being incorrect for the gadolinium tubes.

The variation in the field due to faulty positioning of the gadolinium tubes was found to be ±100 gauss (0.3%). Exact values for the field to within ±0.1% could thus be calculated from the atomic beam measured g-values, provided the corresponding Zeeman patterns could be found on every spectrogram. This was found to be possible; indeed it was possible to find a number of such patterns, yielding a field of greater reliability.

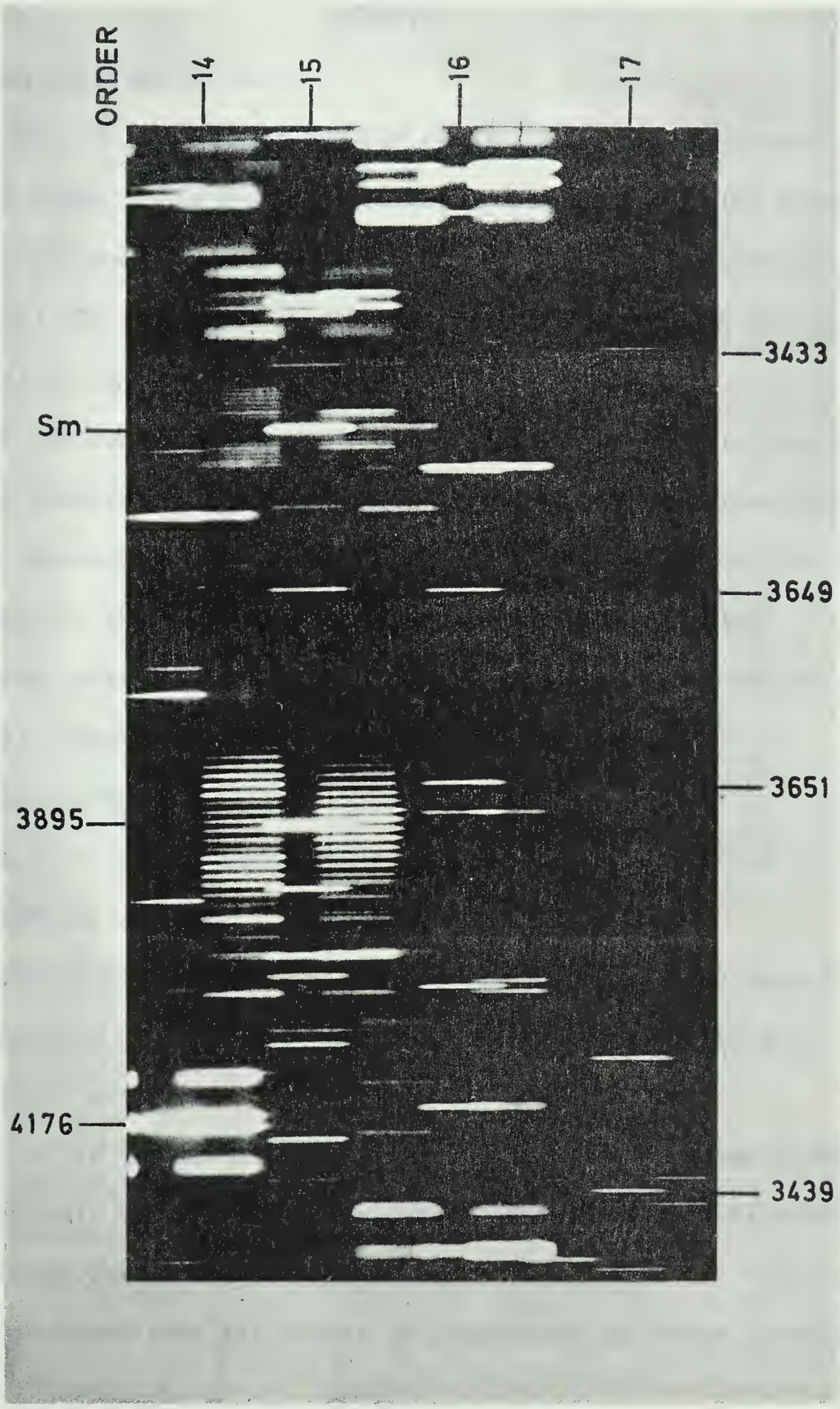

FIG. 1.8 ZEEMAN EFFECT IN GD II

CHAPTER III

RESULTS

3.1 Zeeman Patterns in Gd II

Table 3.1 (p. 27) gives the results for 120 independent Zeeman patterns involving 86 different spectrum lines. The wavelengths are those given by King (Ki 43) and the transitions are from Russel (Ru 50). The weight assigned to each pattern was based on the following scheme:

I: poor pattern: over exposed; too faint; few measurable components

II: fair pattern: partially masked; agreement between calculated and observed displacements fair; measurable components may be good, but they are few in number; π components missing

III: average pattern: agreement between calculated and observed displacements is good on the average, but may be off for certain components

IV: good pattern: agreement between calculated and observed displacements is good.

V: excellent pattern:pattern is well resolved with many measurable components both π and σ; agreement between calculated and observed displacements excellent

Patterns 117 to 120 involve transitions which have not been classified by Russel, but for which the Zeeman patterns were sufficiently well resolved that J values of the levels involved in the transition could be inferred from the number of components and their intensity.

TABLE 3.1 ZEEMAN PATTERNS OBSERVED IN GD II

Nos	Wavelength	Transition	Weight	Pattern
1	3010.129	$a^{10}D^{o}_{5/2}$ -- $y^{10}P_{7/2}$	III	(0.197, 0.597, 0.999) 1.157, 1.545, 1.942, 2.342, 2.740, 3.135
2	3068.643	$a^{10}D^{o}_{9/2}$ -- $y^{10}P_{7/2}$	IV	(0.142, 0.427, 0.723, 1.003) 0.857, 1.143, 1.434, 1.722, 2.008 2.293, 2.593
3	3076.925	$a^{10}D^{o}_{5/2}$ -- $z^{8}F_{7/2}$	V	(o.376, 1.129, 1.894)-0.083, 0.660, 1.411, 2.153, 2.908
4	3089.954	$a^{6}D^{o}_{7/2}$ -- $y^{6}P_{5/2}$	II	0.905, 1.183, 1.427
5	3092.058	$a^{6}D^{o}_{5/2}$ -- $y^{6}P_{3/2}$	I	(0.373, 1.102) 0.539, 1.305
6	3098.644	$a^{10}D^{o}_{5/2}$ -- $y^{8}P_{7/2}$	III	(0.406, 1.221, 2.032)-0.322, 0.509, 1.330, 2.181, 2.991, 3.864
7	3119.941	$a^{10}D^{o}_{7/2}$ -- $y^{8}P_{9/2}$	V	(0.167, 0.500, 0.833, 1.181) 0.577, 0.908, 1.239, 1.575, 1.907 2.247, 2.578
8	3119.941	$a^{10}D^{o}_{7/2}$ -- $y^{8}P_{9/2}$	III	(0.173, 0.519, 0.833, 1.219) 0.579, 0.911, 1.240, 1.577, 1.900
9	3123.989	$a^{10}D^{o}_{7/2}$ -- $y^{8}P_{7/2}$	IV	(0.860, 1.202) 0.880, 1.229, 1.578, 1.923, 2.242, 2.584, 2.906
10	3123.989	$a^{10}D^{o}_{7/2}$ -- $y^{8}P_{7/2}$	IV	(0.517, 0.848, 1.197) 0.870, 1.227, 1.571, 1.907, 2.239, 2.575 2.920
11	3130.812	$b^{8}D^{o}_{5/2}$ -- $y^{8}F_{5/2}$	IV	(0.553, 0.925) 1.134, 1.518, 1.878, 2.243, 2.619
12	3133.094	$a^{10}D^{o}_{5/2}$ -- $z^{6}P_{7/2}$	IV	(0.344, 1.044, 1.736) 0.114, 0.832, 1.516

Nos	Wavelength	Transition	Weight	Pattern
13	3145.516	$b\,^8D^o_{7/2}$ -- $y\,^8F_{9/2}$	II	(0.097, 0.340, 0.584, 0.806) 0.751, 0.985, 1.191, 1.434, 1.680 1.913
14	3146.878	$b\,^8D^o_{5/2}$ -- $y\,^8F_{7/2}$	I	(0.217, 0.654, 1.083) 0.518, 0.947, 1.383, 1.846
15	3268.335	$a\,^{10}D^o_{7/2}$ -- $z\,^8P_{9/2}$	I	0.759, 1.040, 1.352
16	3268.335	$a\,^{10}D^o_{7/2}$ -- $z\,^8P_{9/2}$	IV	(0.146, 0.447, 0.734, 1.043) 0.748, 1.044, 1.338, 1.634, 1.936
17	3331.383	$a\,^{10}D^o_{5/2}$ -- $z\,^8D_{7/2}$	V	(0.362, 1.090, 1.813) ....., 0.743, 1.465, 2.191, 2.927
18	3336.180	$a\,^{10}D^o_{5/2}$ -- $z\,^8D_{5/2}$	IV	(0.788, 1.293) 1.779, 2.304, 2.821, 3.337
19	3345.985	$a\,^{10}D^o_{5/2}$ -- $z\,^8D_{3/2}$	IV	(0.139, 0.410) 2.152, 2.418, 2.698, 2.976
20	3358.620	$a\,^{10}D^o_{7/2}$ -- $z\,^8D_{9/2}$	II	(0.162, 0.498) ....., ..., ..., 1.605, 1.928, 2.242, 2.562, 2.901
21	3360.711	$a\,^{10}D^o_{7/2}$ -- $z\,^8D_{7/2}$	V	(0.642, 0.879) 1.206, 1.454, 1.713, 1.958, 2.211, 2.460, 2.708
22	3399.991	$a\,^8D^o_{3/2}$ -- $z\,^8F_{5/2}$	IV	(0.313, 0.938) 1.242, 1.860, 2.493
23	3399.991	$a\,^8D^o_{3/2}$ -- $z\,^8F_{5/2}$	IV	(0.312, 0.948) 1.238, 1.863, 2.502
24	3405.038	$a\,^6D^o_{3/2}$ -- $z\,^6D_{1/2}$	II	(1.158) 3.060
25	3413.273	$a\,^6D^o_{3/2}$ -- $z\,^6D_{3/2}$	II	(1.013) 0.885, 1.519, 2.176
26	3416.948	$a\,^8D^o_{7/2}$ -- $z\,^8F_{9/2}$	III	(0.134, 0.394, 0.642, 0.890) 0.731, 0.971, 1.239, 1.473, 1.741 2.001

Nos	Wavelength	Transition	Weight	Pattern
27	3416.948	$a^8D^o_{7/2}$ -- $z^8F_{9/2}$	III	(0.128, 0.382, 0.633, 0.869) 0.738, 0.959, 1.228, 1.492, 1.740 1.998
28	3418.733	$a^{10}D^o_{5/2}$ -- $z^{10}D_{7/2}$	IV	(0.317, 0.929, 1.538) 0.411, 1.016, 1.631, 2.255, 2.866, 3.464
29	3418.733	$a^{10}D^o_{5/2}$ -- $z^{10}D_{7/2}$	IV	(0.313, 0.922, 1.527) 0.410, 1.021, 1.631, 2.252, 2.854, 3.487
30	3423.92	$a^{10}D^o_{5/2}$ -- $z^{10}D_{5/2}$	III	(0.403, 0.638) 1.906, 2.170, 2.405, 2.661, 2.909
31	3424.592	$a^8D^o_{3/2}$ -- $z^8F_{3/2}$	III	(0.395, 1.199) 1.650, 2.402, 3.201
32	3425.930	$a^8D^o_{5/2}$ -- $y^8P_{7/2}$	IV	(0.151, 0.458, 0.762) 0.978, 1.300, 1.603, 1.890
33	3425.930	$a^8D^o_{5/2}$ -- $y^8P_{7/2}$	III	(0.147, 0.446, 0.753) 0.976, 1.286, 1.598, 1.901
34	3439.208	$a^8D^o_{5/2}$ -- $y^8P_{5/2}$	III	(0.353, 0.582) 1.458, 1.705, 1.919, 2.163, 2.398
35	3454.904	$a^{10}D^o_{7/2}$ -- $z^{10}D_{5/2}$	IV	(0.102, 0.329, 0.540) 1.562, 1.773, 1.991, 2.210, 2.429
36	3467.267	$a^8D^o_{7/2}$ -- $z^8F_{5/2}$	IV	(0.149, 0.440, 0.746) 1.131, 1.420, 1.719, 2.013, 2.311, 2.585
37	3467.267	$a^8D^o_{7/2}$ -- $z^8F_{5/2}$	II	(0.132, 0.428, 0.732) 1.106, 1.417, 1.725, 2.007, 2.335
38	3473.219	$a^{10}D^o_{7/2}$ -- $z^{10}D_{9/2}$	IV	(0.122, 0.382, 0.658) 0.909, ..., 1.423, 1.673, 1.951, 2.202 2.484
39	3473.219	$a^{10}D^o_{7/2}$ -- $z^{10}D_{9/2}$	IV	(0.130, 0.388, 0.649, 0.910) 0.907, 1.161, 1.424, 1.688, 1.951 2.192

Nos	Wavelength	Transition	Weight	Pattern
40	3473.219	$a^{10}D^{o}_{7/2}$ -- $z^{10}D_{9/2}$	IV	(0.130, 0.391, 0.658, 0.905) 0.908, 1.160, 1.424, 1.692, 1.944 2.222
41	3491.954	$a^{10}D^{o}_{5/2}$ -- $4_{5/2}$	I	(0.360, 0.566) 2.036, 2.238, 2.452, 2.680, 2.890
42	3491.954	$a^{10}D^{o}_{5/2}$ -- $4_{5/2}$	II	(0.365, 0.560) 2.022, 2.230, 2.444, 2.661, 2.875
43	3491.954	$a^{10}D^{o}_{5/2}$ -- $4_{5/2}$	II	(0.559) 2.238, 2.461, 2.673
44	3524.196	$a^{10}D^{o}_{7/2}$ -- $4_{5/2}$	III	(0.118, 0.360, 0.620) 1.473, 1.708, 1.957, 2.185
45	3524.196	$a^{10}D^{o}_{7/2}$ -- $4_{5/2}$	IV	(0.121, 0.361, 0.597) 1.467, 1.719, 1.946
46	3544.985	$a^{10}F^{o}_{7/2}$ -- $z^{8}F_{9/2}$	II	(0.142, 0.409) 0.676, 0.951, 1.225, 1.496, 1.754
47	3571.933	$a^{10}D^{o}_{5/2}$ -- $z^{8}P_{7/2}$	I	....., ..., ..., 2.258, 2.867
48	3608.753	$b^{8}D^{o}_{7/2}$ -- $y^{8}D_{5/2}$	III	(0.107, 0.329, 0.544) 1.251, 1.457, 1.692, 1.921
49	3608.753	$b^{8}D^{o}_{7/2}$ -- $y^{8}D_{5/2}$	IV	(0.107, 0.329, 0.555) 1.252, 1.473, 1.693, 1.913, 2.135
50	3613.392	$b^{8}D^{o}_{5/2}$ -- $y^{8}D_{3/2}$	III	(0.351) 1.016, 1.705, 2.394
51	3649.44	$b^{8}D^{o}_{3/2}$ -- $y^{8}D_{5/2}$	II	(0.375, 1.108) 0.906, 1.664, 2.426
52	3650.95	$b^{8}D^{o}_{5/2}$ -- $y^{8}D_{7/2}$	I	(0.126, 0.398, 0.631) 1.113, 1.404, 1.649, 1.921, 2.206
53	3662.26	$a^{10}D^{o}_{5/2}$ -- $z^{8}P_{5/2}$	IV	(0.314, 0.500) 2.063, 2.263, 2.457, 2.659, 2.852
54	3671.20	$a^{10}D^{o}_{9/2}$ -- $z^{10}F_{11/2}$	IV	(0.108, 0.290, 0.500, 0.726, 0.882) 0.765, 0.944, 1.154, 1.353 1.557, 1.752

Nos	Wavelength	Transition	Weight	Pattern
55	3671.20	$a^{10}D^{o}_{9/2}$ -- $z^{10}F_{11/2}$	V	(0.101, 0.301, 0.499, 0.720, 0.901) 0.757, 0.946, 1.157, 1.358, 1.559, 1.752, 1.960, 2.159
56	3687.74	$a^{8}D^{o}_{3/2}$ -- $z^{8}D_{5/2}$	III	(0.373, 1.120) 0.909, 1.659, 2.419, 3.184
57	3697.73	$a^{10}D^{o}_{7/2}$ -- $z^{8}P_{5/2}$	III	(0.122, 0.412, 0.674) 1.413, 1.671, 1.945, 2.225, 2.494, 2.803
58	3697.73	$a^{10}D^{o}_{7/2}$ -- $z^{8}P_{5/2}$	III	(0.127, 0.408, 0.679) 1.416, 1.679, 1.943, 2.229, 2.492, 2.813
59	3697.73	$a^{10}D^{o}_{7/2}$ -- $z^{8}P_{5/2}$	IV	(0.133, 0.403, 0.671) 1.405, 1.670, 1.957, 2.210, 2.472, 2.772
60	3712.70	$a^{8}D^{o}_{5/2}$ -- $z^{8}D_{7/2}$	III	(0.098, 0.318, 0.535) 1.302, 1.506, 1.734, 1.907, 2.124
61	3716.36	$a^{10}D^{o}_{7/2}$ -- $z^{10}F_{9/2}$	IV	(0.178, 0.524, 0.879, 1.242) 0.493, 0.845, 1.203, 1.555, 1.910, 2.276, 2.624
62	3716.36	$a^{10}D^{o}_{7/2}$ -- $z^{10}F_{9/2}$	I	(0.178) ....., ..., ..., 1.549, 1.908, 2.258, 2.593
63	3716.36	$a^{10}D^{o}_{7/2}$ -- $z^{10}F_{9/2}$	III	(0.172, 0.510, 0.863, 1..212) 0.494 0.841, 1.192, 1.545, 1.904 2.255, 2.613, 2.997
64	3730.84	$a^{8}D^{o}_{5/2}$ -- $z^{8}D_{3/2}$	V	(0.396, 1.179) 0.870, 1.653, 2.441, 3.228
65	3730.84	$a^{8}D^{o}_{5/2}$ -- $z^{8}D_{3/2}$	V	(0.396, 1.181) 0.867, 1.654, 2.441, 3.228
66	3730.84	$a^{8}D^{o}_{5/2}$ -- $z^{8}D_{3/2}$	V	(0.394, 1.183) 0.866, 1.654, 2.450, 3.252
67	3759.00	$a^{10}D^{o}_{5/2}$ -- $z^{10}F_{7/2}$	IV	(0.342, 1.041, 1.726) 0.108, 0.818, 1.516, 2.226, 2.902
68	3796.37	$a^{10}D^{o}_{7/2}$ -- $z^{10}F_{7/2}$	IV	(0.353, 0.576, 0.777) 1.317, 1.542, 1.758, 1.975, 2.188, 2.386 2.614

Nos	Wavelength	Transition	Weight	Pattern
69	3796.37	$a^{10}D^{o}_{7/2}$ -- $z^{10}F_{7/2}$	II	1.323, 1.562, 1.766, <u>1.978</u>, 2.198, 2.394, 2.610
70	3813.97	$a^{10}D^{o}_{5/2}$ -- $z^{10}F_{5/2}$	IV	(0.191, 0.588, <u>0.974</u>) 1.587, 1.976, <u>2.365</u>, 2.760, 3.144
71	3813.97	$a^{10}D^{o}_{5/2}$ -- $z^{10}F_{5/2}$	V	(0.587, <u>0.973</u>) 1.584, 1.974, <u>2.361</u>, 2.753, 3.137
72	3816.64	$a^{10}D^{o}_{7/2}$ -- $z^{10}P_{9/2}$	II	(<u>0.117</u>, 0.402, 0.677) <u>0.894</u>, 1.146, 1.411, 1.680, 1.954, 2.232
73	3816.64	$a^{10}D^{o}_{7/2}$ -- $z^{10}P_{9/2}$	III	(<u>0.134</u>, 0.402, 0.674) <u>0.892</u>, 1.139, 1.414, 1.680
74	3850.97	$a^{10}D^{o}_{5/2}$ -- $z^{10}F_{3/2}$	IV	(<u>0.267</u>, 0.808) <u>1.747</u>, 2.293, 2.824
75	3850.97	$a^{10}D^{o}_{5/2}$ -- $z^{10}F_{3/2}$	III	(<u>0.259</u>, 0.800) <u>1.746</u>, 2.284, 2.823, 3.362
76	3850.97	$a^{10}D^{o}_{5/2}$ -- $z^{10}F_{3/2}$	II	<u>1.740</u>, 2.286, 2.822, 3.350
77	3875.46	$a^{10}F^{o}_{5/2}$ -- $z^{8}D_{7/2}$	III	(<u>0.182</u>, 0.564, 0.918) <u>0.906</u>, 1.280, 1.652, 2.031
78	3881.84	$a^{8}S^{o}_{7/2}$ -- $z^{10}D_{5/2}$	I	(0.579, <u>0.945</u>) <u>0.945</u>, 1.346
79	3894.696	$a^{10}D^{o}_{5/2}$ -- $z^{10}P_{7/2}$	IV	(<u>0.177</u>, 0.557, 0.935) <u>1.260</u>, 1.632, 2.003, 2.379, 2.749
80	3894.696	$a^{10}D^{o}_{5/2}$ -- $z^{10}P_{7/2}$	V	(<u>0.184</u>, 0.560, 0.932) <u>1.257</u>, 1.628, 1.998, 2.366, 2.747, 3.150
81	3923.346	$a^{10}F^{o}_{7/2}$ -- $z^{8}D_{5/2}$	II	(<u>0.075</u>, 0.228, 0.367) <u>1.521</u>, 1.664, 1.784, 1.942, 2.085
82	3971.754	$a^{10}F^{o}_{3/2}$ -- $z^{10}D_{5/2}$	IV	(<u>0.427</u>, 1.281) <u>1.031</u>, 1.879, 2.739
83	3993.213	$a^{10}D^{o}_{9/2}$ -- $z^{10}P_{7/2}$	III	(<u>.....</u>, 0.481, 0.777, 1.098) <u>0.758</u>, 1.070, 1.402, 1.719
84	3994.165	$a^{10}F^{o}_{5/2}$ -- $z^{10}D_{7/2}$	IV	(<u>0.128</u>, 0.392, 0.659) <u>1.309</u>, 1.565, 1.806, 2.076
85	4140.450	$a^{10}F^{o}_{7/2}$ -- $4_{5/2}$	IV	(<u>0.220</u>, 0.669, 1.107) <u>0.782</u>, 1.227, 1.659, 2.107

Nos	Wavelength	Transition	Weight	Pattern
86	4153.510	$a^8F^o_{5/2}$ -- $y^8D_{5/2}$	IV	(0.504, 0.826) 1.217, 1.540, 1.871, 2.197, 2.530
87	4162.732	$a^8D^o_{9/2}$ -- $z^8P_{7/2}$	III	(0.083, 0.391, 0.664) 0.758, 1.018, 1.283, 1.548, 1.813
88	4162.732	$a^8D^o_{9/2}$ -- $z^8P_{7/2}$	IV	(0.129, 0.398, 0.666, 0.930) 0.763, 1.024, 1.295, 1.551, 1.823 2.074
89	4173.556	$a^8F^o_{7/2}$ -- $y^8D_{5/2}$	V	(0.211, 0.630, 1.052) 0.556, 0.974, 1.398, 1.817
90	4204.857	$a^{10}F^o_{5/2}$ -- $z^8P_{7/2}$	V	(0.125, 0.377, 0.631) 1.317, 1.569, 1.816, 2.071, 2.339
91	4204.857	$a^{10}F^o_{5/2}$ -- $z^8P_{7/2}$	V	(0.126, 0.378, 0.633) 1.316, 1.569, 1.820, 2.076
92	4215.023	$a^8S^o_{7/2}$ -- $z^{10}F_{9/2}$	II	(0.087, 0.271, 0.428) 1.122, 1.317, 1.512, 1.680
93	4217.195	$a^{10}F^o_{11/2}$-- $z^{10}D_{9/2}$	IV	(0.075, 0.230, 0.381, 0.528, 0.686) 0.969, 1.123, 1.272, 1.423, 1.582, 1.734
94	4217.195	$a^{10}F^o_{11/2}$-- $z^{10}D_{9/2}$	V	(0.076, 0.229, 0.384, 0.540, 0.688) 0.970, 1.127, 1.278, 1.429 1.571
95	4229.803	$a^8F^o_{9/2}$ -- $y^8D_{7/2}$	III	(0.108, 0.328, 0.552, 0.781) 0.799, 1.014, 1.244
96	4251.733	$a^8D^o_{5/2}$ -- $z^{10}F_{7/2}$	IV	(0.094, 0.279) 1.401, 1.584, 1.766
97	4251.733	$a^8D^o_{5/2}$ -- $z^{10}F_{7/2}$	III	(0.088, 0.265) 1.399, 1.576, 1.754, 1.944, 2.149
98	4280.490	$a^8D^o_{3/2}$ -- $z^{10}F_{5/2}$	V	(0.315, 0.951) 1.225, 1.854, 2.485
99	4280.490	$a^8D^o_{3/2}$ -- $z^{10}F_{5/2}$	V	(0.314, 0.944) 1.227, 1.856, 2.488

Nos	Wavelength	Transition	Weight	Pattern
100	4280.490	$a^8D^o_{3/2}$ -- $z^{10}F_{5/2}$	IV	(0.315, 0.950) 1.222, 1.859, 2.482, 3.120
101	4296.076	$a^{10}F^o_{3/2}$ -- $z^8P_{5/2}$	IV	(0.399) 1.167, 1.965, 2.758
102	4408.248	$a^{10}F^o_{7/2}$ -- $z^{10}F_{9/2}$	V	1.168, 1.325, 1.491, 1.651
103	4419.032	$a^8D^o_{9/2}$ -- $z^{10}F_{7/2}$	I	1.082, 1.244, 1.438, 1.619
104	4466.547	$a^{10}F^o_{5/2}$ -- $z^{10}F_{7/2}$	II	(0.174, 0.511) 1.007, 1.340, 1.677, 2.035, 2.385
105	4471.29	$a^6D^o_{7/2}$ -- $z^6P_{5/2}$	III	(0.163, 0.522, 0.853) 0.756, 1.092, 1.433, 1.767
106	4514.505	$a^{10}P^o_{9/2}$ -- $y^{10}P_{7/2}$	III	(....., 0.333, 0.559, 0.773) 1.197, 1.413, 1.619, 1.844, 2.059
107	4558.080	$a^{10}F^o_{3/2}$ -- $z^{10}F_{3/2}$	II	(0.076) 3.125
108	4596.978	$a^{10}F^o_{5/2}$ -- $z^{10}F_{3/2}$	III	(0.450, 1.336) 0.869, 1.759
109	4601.05	$a^{10}F^o_{7/2}$ -- $z^{10}F_{5/2}$	IV	(0.139, 0.423) 1.188, 1.471
110	4865.02	$b^8D^o_{5/2}$ -- $z^8D_{3/2}$	IV	(0.394, 1.179) 0.874, 1.658
111	5125.56	$a^{10}P^o_{11/2}$ -- $z^{10}D_{13/2}$	I	0.973, 1.098, 1.240, 1.352
112	5186.915	$a^8F^o_{3/2}$ -- $z^8F_{1/2}$	I	(0.886) 0.955, 2.962
113	5187.237	$a^8F^o_{5/2}$ -- $z^8F_{3/2}$	II	(0.155, 0.422) 1.273, 1.588
114	5220.297	$a^6D^o_{9/2}$ -- $z^{10}D_{7/2}$	I	(0.197) 0.182, 0.600, 0.905
115	5583.68	$b^8D^o_{11/2}$ -- $z^{10}P_{9/2}$	II	0.855, 1.029, 1.205, 1.389, 1.569, 1.747
116	5733.86	$a^{10}P^o_{9/2}$ -- $z^{10}P_{11/2}$	II	1.008, 1.176, 1.354, 1.524, 1.702, 1.870

Unidentified Transitions

Nos	Wavelength	Transition	Pattern
117	3364.241	5/2? -- 5/2?	1.032, 2.146, 2.991
118	3622.810	11/2? -- 9/2?	(0.126, 0.387, 0.643, 0.891) 0.444, 0.681, 0.965, 1.193, 1.455
119	3622.810	11/2? -- 9/2?	(0.121, 0.391, 0.641, 0.887) 0.443, 0.696, 0.955, 1.197, 1.476
120	3694.03	7/2? -- 5/2?	(0.186, 0.607, 0.980) 0.670, 1.061, 1.448

3.2 Individual g-Values Obtained for Gd II

Table 3.2 gives the 232 g-values calculated from Zeeman patterns for which the transitions had been classified. The weight assigned to each pattern has been explained previously (p. 26). The calculation of the g-values is explained in Appendix A-3 (p.63). The final g-value given is the weighted mean of the observations, with the error being calculated according to the following scheme, with exceptions depending on whether the pattern was particularly good or generally poor:

Number of observations	Error
a) Single result	
- if pattern is good	±.007
- if pattern is fair	±.01
- if pattern is poor	±.02
b) Two results	
- if patterns are good	±.005
- if patterns are fair	±.01 to ±.007
c) Three results	±.004
d) Four results	standard error (unless spread is large)
e) Five results	standard error

The standard error of the weighted mean e was calculated from the formula (To 55):

$$e = \left| \frac{\Sigma W_s (g_s - \bar{g})^2}{(n - 1)\Sigma W_s} \right|^{\frac{1}{2}}$$

where W_s = weight assigned to each pattern, $g_s - \bar{g}$ = variation of each calculated g-value from the weighted mean, and n = number of observations (4 or greater).

TABLE 3.2

g-VALUES OBTAINED FOR ENERGY LEVELS IN GD II

Odd Levels

Level	Wavelength	Weight	g-Value	Final Value
$a\,^{10}D^{o}_{5/2}$	3010.129	III	2.547	2.557±.0012
	3076.925	V	2.545	(23 obs)
	3098.644	III	2.565	
	3133.094	IV	2.550	
	3331.383	V	2.556	
	3336.180	IV	2.563	
	3345.985	IV	2.565	
	3418.733	IV	2.564	
	3418.733	IV	2.557	
	3423.92	III	2.553	
	3491.954	I	2.560	
	3491.954	II	2.566	
	3491.954	II	2.554	
	3571.933	I	2.563	
	3662.26	IV	2.555	
	3759.00	V	2.556	
	3813.97	V	2.556	
	3813.97	IV	2.561	
	3850.97	III	2.555	
	3850.97	IV	2.554	
	3850.97	III	2.553	
	3894.696	V	2.556	
	3894.696	IV	2.559	
$a\,^{10}D^{o}_{7/2}$	3119.941	III	2.078	2.082±.0014
	3119.941	V	2.080	(24 obs)
	3123.989	IV	2.085	
	3123.989	IV	2.081	
	3268.335	IV	2.075	

Level	Wavelength	Weight	g-Value	Final Value
$a\,^{10}D^{o}_{7/2}$ contd.	3268.335	I	2.096	
	3358.620	II	2.093	
	3360.711	V	2.084	
	3454.904	IV	2.100	
	3473.219	IV	2.079	
	3473.219	IV	2.079	
	3473.219	IV	2.079	
	3524.196	III	2.071	
	3524.196	IV	2.070	
	3697.73	III	2.088	
	3697.73	IV	2.080	
	3697.73	III	2.080	
	3716.36	IV	2.088	
	3716.36	I	2.083	
	3716.36	III	2.075	
	3796.37	IV	2.084	
	3796.37	II	2.084	
	3816.64	II	2.091	
	3816.64	III	2.084	
$a\,^{10}D^{o}_{9/2}$	3068.643	IV	1.863	1.860±.0017
	3671.20	V	1.857	(4 obs)
	3671.20	IV	1.858	
	3993.213	III	1.864	
$a\,^{8}D^{o}_{3/2}$	3399.991	IV	2.805	2.803±.0022
	3399.991	IV	2.813	(7 obs)
	3424.592	III	2.800	
	3687.74	III	2.793	
	4280.490	IV	2.807	

Level	Wavelength	Weight	g-Value	Final Value
$a\,^8D^o_{3/2}$ contd.	4280.490	V	2.800	
	4280.490	V	2.800	
$a\,^8D^o_{5/2}$	3425.930	IV	2.046	2.044±.0025
	3425.930	III	2.044	(9 obs)
	3439.208	III	2.036	
	3712.70	III	2.037	
	3730.84	V	2.047	
	3730.84	V	2.048	
	3730.84	V	2.050	
	4251.733	III	2.026	
	4251.733	IV	2.049	
$a\,^8D^o_{7/2}$	3416.948	III	1.872	1.870±.003
	3416.948	III	1.874	(4 obs)
	3467.267	IV	1.871	
	3467.267	II	1.860	
$a\,^8D^o_{9/2}$	4162.732	IV	1.691	1.69±.01
	4162.732	III	1.686	(3 obs)
	4419.032	I	1.860	
$a\,^{10}F^o_{3/2}$	3971.754	IV	3.166	3.163±.005
	4296.076	IV	3.162	(3 obs)
	4558.080	II	3.157	
$a\,^{10}F^o_{5/2}$	3875.46	III	2.210	2.205±.0038
	3994.165	IV	2.219	(6 obs)
	4204.857	V	2.196	
	4204.857	V	2.198	

Level	Wavelength	Weight	g-Value	Final Value
$a\,^{10}F^{o}_{5/2}$ contd.	4466.547	II	2.205	
	4596.978	III	2.210	
$a\,^{10}F^{o}_{7/2}$	3544.985	II	1.905	1.894±.0023
	3923.246	II	1.896	(5 obs)
	4140.450	IV	1.890	
	4408.248	V	1.893	
	4601.05	IV	1.891	
$a\,^{10}F^{o}_{11/2}$	4217.195	V	1.661	1.657±.005
	4217.195	IV	1.653	(2 obs)
$b\,^{8}D^{o}_{11/2}$	5583.68	II	1.640	1.64±.02
$b\,^{8}D^{o}_{7/2}$	3145.516	II	1.786	1.794±.004
	3608.753	III	1.794	(3 obs)
	3608.753	IV	1.797	
$b\,^{8}D^{o}_{5/2}$	3130.812	IV	2.063	2.055±.0036
	3146.878	I	2.037	(5 obs)
	3613.392	III	2.052	
	3650.95	I	2.047	
	4865.02	IV	2.055	
$b\,^{8}D^{o}_{3/2}$	3649.44	II	2.781	2.78±.02
$a\,^{6}D^{o}_{9/2}$	5220.297	I	1.564	1.56±.02
$a\,^{6}D^{o}_{7/2}$	3089.954	II	1.558	1.59 ±.01
	4471.29	III	1.601	(2 obs)

Level	Wavelength	Weight	g-Value	Final Value
$a^6D^o_{5/2}$	3092.058	I	1.658	1.66±.02
$a^6D^o_{3/2}$	3405.038	II	1.902	1.88±.02
	3413.273	II	1.857	(2 obs)
$a^{10}P^o_{9/2}$	4514.505	III	1.953	1.94±.01
	5133.86	II	1.935	(2 obs)
$a^{10}P^o_{11/2}$	5125.56	I	1.773	1.77±.02
$a^8F^o_{3/2}$	5186.915	I	1.958	1.96±.02
$a^8F^o_{5/2}$	4153.510	IV	1.707	1.709±.005
	5187.237	II	1.715	(2 obs)
$a^8F^o_{7/2}$	4173.556	V	1.609	1.609±.007
$a^8F^o_{9/2}$	4229.803	III	1.566	1.57±.01
$a^8S^o_{7/2}$	3881.84	I	1.90	1.91±.01
	4215.023	II	1.910	(2 obs)
		EVEN LEVELS		
$z^{10}P_{7/2}$	3894.696	V	2.185	2.185±.003
	3894.696	IV	2.188	(3 obs)
	3993.213	III	2.180	
$z^{10}P_{9/2}$	3816.64	II	1.821	1.818±.005
	3816.64	III	1.816	(3 obs)
	5583.68	II	1.817	
$z^{10}P_{11/2}$	5733.86	II	1.764	1.76±.02

Level	Wavelength	Weight	g-Value	Final Value
$z\,^{10}F_{3/2}$	3850.97	IV	3.092	3.094±.0024
	3850.97	II	3.092	(5 obs)
	3850.97	III	3.091	
	4558.080	III	3.093	
	4596.978	III	3.104	
$z\,^{10}F_{5/2}$	3813.97	IV	2.170	2.171±.001
	3813.97	V	2.167	(6 obs)
	4280.490	IV	2.175	
	4280.490	V	2.171	
	4280.490	V	2.170	
	4601.05	IV	2.172	
$z\,^{10}F_{7/2}$	3759.00	V	1.861	1.862±.0039
	3796.37	II	1.872	(7 obs)
	3796.37	IV	1.864	
	4251.733	III	1.846	
	4251.733	IV	1.864	
	4419.032	I	1.888	
	4466.547	II	1.859	
$z\,^{10}F_{9/2}$	3716.36	IV	1.734	1.731±.0023
	3716.36	I	1.728	(5 obs)
	3716.36	III	1.722	
	4215.023	II	1.735	
	4408.248	V	1.732	
$z\,^{10}F_{11/2}$	3671.20	IV	1.657	1.657±.005
	3671.20	V	1.657	(2 obs)

Level	Wavelength	Weight	g-Value	Final Value
$z\,^8P_{5/2}$	3662.26	IV	2.360	2.536±.0032
	3697.73	III	2.358	(5 obs)
	3697.73	III	2.347	
	3697.73	IV	2.350	
	4296.076	IV	2.364	
$z\,^8P_{7/2}$	3571.933	I	1.954	1.949±.0023
	4162.732	IV	1.955	(5 obs)
	4162.732	III	1.951	
	4204.857	V	1.945	
	4204.857	V	1.946	
$z\,^8P_{9/2}$	3268.335	IV	1.780	1.784±.007
	3268.335	I	1.799	(2 obs)
$z\,^{10}D_{5/2}$	3423.92	III	2.298	2.308±.0066
	3454.904	IV	2.318	(4 obs)
	3881.84	I	2.28	
	3971.754	IV	2.312	
$z\,^{10}D_{7/2}$	3418.733	IV	1.949	1.951±.0031
	3418.733	IV	1.946	(4 obs)
	3994.165	IV	1.959	
	5220.297	I	1.953	
$z\,^{10}D_{9/2}$	3473.219	IV	1.817	1.812±.0027
	3473.219	IV	1.819	(5 obs)
	3473.219	IV	1.819	
	4217.195	V	1.814	
	4217.195	IV	1.805	

Level	Wavelength	Weight	g-Value	Final Value
$z^{10}D_{13/2}$	5125.56	I	1.648	1.65±.02
$z^{8}D_{3/2}$	3345.985	IV	2.840	2.838±.0011
	3730.84	V	2.837	(5 obs)
	3730.84	V	2.835	
	3730.84	V	2.839	
	4865.02	IV	2.842	
$z^{8}D_{5/2}$	3336.180	IV	2.046	2.043±.004
	3687.74	III	2.037	(3 obs)
	3923.246	II	2.046	
$z^{8}D_{7/2}$	3331.383	V	1.831	1.832±.003
	3360.711	V	1.833	(4 obs)
	3712.70	III	1.827	
	3875.46	III	1.838	
$z^{8}D_{9/2}$	3358.620	II	1.768	1.77±.02
$y^{8}P_{5/2}$	3439.208	III	1.802	1.80±.02
$y^{8}P_{7/2}$	3098.644	III	1.737	1.743±.0019
	3123.989	IV	1.747	(5 obs)
	3123.989	IV	1.741	
	3425.930	IV	1.741	
	3425.930	III	1.747	
$y^{8}P_{9/2}$	3119.941	III	1.745	1.746±.005
	3119.941	V	1.746	(2 obs)
$z^{6}P_{7/2}$	3133.094	IV	1.854	1.85±.01

Level	Wavelength	Weight	g-Value	Final Value
$z^6P_{5/2}$	4471.29	III	1.939	1.94±.01
$z^8F_{1/2}$	5186.915	I	3.966	3.97±.02
$z^8F_{3/2}$	3424.592	III	2.005	2.01±.01
	5187.237	III	2.021	(2 obs)
$z^8F_{5/2}$	3399.991	IV	2.180	2.173±.006
	3399.991	IV	2.183	(4 obs)
	3467.267	IV	2.167	
	3467.267	III	2.156	
$z^8F_{7/2}$	3076.925	V	1.791	1.791±.007
$z^8F_{9/2}$	3416.948	III	1.619	1.622±.004
	3416.948	III	1.619	(3 obs)
	3544.985	II	1.632	
$y^{10}P_{7/2}$	3010.129	III	2.150	2.155±.0064
	3068.643	IV	2.149	(3 obs)
	4514.505	III	2.169	
$y^8D_{7/2}$	3650.95	I	1.795	1.79±.01
	4229.803	III	1.785	(2 obs)
$y^8D_{5/2}$	3608.753	IV	2.015	2.025±.0047
	3608.753	III	2.011	(5 obs)
	3649.44	II	2.031	
	4153.510	IV	2.035	
	4173.556	V	2.030	

Level	Wavelength	Weight	g-Value	Final Value
$y^8D_{3/2}$	3613.392	III	2.745	2.745±.01
$z^6D_{3/2}$	3413.273	II	1.181	1.18±.02
$z^6D_{1/2}$	3405.08	II	-0.414	-0.41±.02
$y^8F_{9/2}$	3145.516	II	1.556	1.56±.02
$y^8F_{7/2}$	3146.878	I	1.603	1.60±.02
$y^8F_{5/2}$	3130.812	IV	1.693	1.69±.01
$y^6P_{5/2}$	3089.954	II	1.819	1.82±.02
$y^6P_{3/2}$	3092.058	I	2.404	2.40±.02
$^4_{5/2}$	3491.954	I	2.34	2.325±.0058
	3491.954	II	2.338	(6 obs)
	3491.954	II	2.340	
	3524.196	III	2.310	
	3524.196	IV	2.311	
	4140.450	IV	2.332	

3.3 Mean g-Values for Gd II

Table 3.3 is a summary of the 67 observed g-values compared with the classical L-S values and those obtained by Smith and Wybourne.

It will be seen that in 80% of the cases, the correction proposed by Smith and Wybourne is in the right direction. In 50% of the cases it is in the right direction but not large enough. For 18% of the cases it agrees with observation within experimental error and for 77% of the cases it agrees within 2% of the observed value.

Those cases where there is marked disagreement between predicted and observed g-values will be discussed in chapter 4, dealing with the analysis of results.

TABLE 3.3

SUMMARY OF g-VALUES IN GD II

Odd Levels

Level	L-S	S-W	Obs.	No. of Obs.
$a^{10}D^o_{5/2}$	2.572	2.570	2.557±.0012	23
$a^{10}D^o_{7/2}$	2.095	2.093	2.082±.0014	24
$a^{10}D^o_{9/2}$	1.879	1.877	1.860±.0017	4
$a^{8}D^o_{3/2}$	2.800	2.827	2.803±.0022	7
$a^{8}D^o_{5/2}$	2.057	2.064	2.044±.0025	9
$a^{8}D^o_{7/2}$	1.809	1.810	1.870±.003	4
$a^{8}D^o_{9/2}$	1.697	1.697	1.69 ±.01	3
$a^{10}F^o_{3/2}$	3.200	3.159	3.163±.005	3
$a^{10}F^o_{5/2}$	2.229	2.211	2.205±.0038	6
$a^{10}F^o_{7/2}$	1.905	1.895	1.894±.0023	5
$a^{10}F^o_{11/2}$	1.678	1.674	1.657±.005	2
$b^{8}D^o_{11/2}$	1.636	1.641	1.64 ±.02	1
$b^{8}D^o_{7/2}$	1.809	1.815	1.794±.004	3
$b^{8}D^o_{5/2}$	2.057	2.058	2.055±.0036	5
$b^{8}D^o_{3/2}$	2.800	2.801	2.78 ±.02	1
$a^{6}D^o_{9/2}$	1.556	1.560	1.56 ±.02	1
$a^{6}D^o_{7/2}$	1.587	1.594	1.59 ±.01	2
$a^{6}D^o_{5/2}$	1.657	1.663	1.66 ±.02	1
$a^{6}D^o_{3/2}$	1.867	1.872	1.88 ±.02	2
$a^{10}P^o_{9/2}$	1.960	1.953	1.94 ±.01	2

Level	L-S	S-W	Obs.	No. of Obs.
$a\,^{10}P^{o}_{11/2}$	1.818	1.808	1.77 ±.02	1
$a\,^{8}F^{o}_{3/2}$	2.000	2.000	1.96 ±.02	1
$a\,^{8}F^{o}_{5/2}$	1.715	1.714	1.709±.005	2
$a\,^{8}F^{o}_{7/2}$	1.619	1.619	1.609±.007	1
$a\,^{8}F^{o}_{9/2}$	1.576	1.576	1.57 ±.01	1
$a\,^{8}S^{o}_{7/2}$	2.000	-----	1.91 ±.01	2
		Even Levels		
$z\,^{10}P_{7/2}$	2.222	2.200	2.185±.003	3
$z\,^{10}P_{9/2}$	1.960	1.925	1.818±.005	3
$z\,^{10}P_{11/2}$	1.818	1.770	1.76 ±.02	1
$z\,^{10}F_{3/2}$	3.200	3.123	3.094±.0024	5
$z\,^{10}F_{5/2}$	2.229	2.185	2.171±.001	6
$z\,^{10}F_{7/2}$	1.905	1.875	1.862±.0039	7
$z\,^{10}F_{9/2}$	1.758	1.738	1.731±.0023	5
$z\,^{10}F_{11/2}$	1.678	1.686	1.657±.005	2
$z\,^{8}P_{5/2}$	2.286	2.373	2.536±.0032	5
$z\,^{8}P_{7/2}$	1.937	1.965	1.949±.0023	5
$z\,^{8}P_{9/2}$	1.778	1.783	1.784±.007	2
$z\,^{10}D_{5/2}$	2.572	2.397	2.308±.0066	4
$z\,^{10}D_{7/2}$	2.095	1.971	1.951±.0031	4
$z\,^{10}D_{9/2}$	1.879	1.818	1.812±.0027	5

Level	L-S	S-W	Obs.	No. of Obs.
$z^{10}D_{13/2}$	1.692	1.674	1.65 ±.02	1
$z^{8}D_{3/2}$	2.800	2.856	2.838±.0011	5
$z^{8}D_{5/2}$	2.057	2.097	2.043±.004	3
$z^{8}D_{7/2}$	1.809	1.849	1.832±.003	4
$z^{8}D_{9/2}$	1.697	1.785	1.77 ±.02	1
$y^{8}P_{5/2}$	2.286	2.238	1.80 ±.02	1
$y^{8}P_{7/2}$	1.937	1.933	1.743±.0019	5
$y^{8}P_{9/2}$	1.778	1.783	1.746±.005	2
$z^{6}P_{7/2}$	1.714	1.807	1.85 ±.01	1
$z^{6}P_{5/2}$	1.886	1.946	1.94 ±.01	1
$z^{8}F_{1/2}$	4.000	3.988	3.97 ±.02	1
$z^{8}F_{3/2}$	2.000	2.007	2.01 ±.01	2
$z^{8}F_{5/2}$	1.714	1.781	2.173±.006	4
$z^{8}F_{7/2}$	1.619	1.653	1.791±.007	1
$z^{8}F_{9/2}$	1.576	1.599	1.622±.004	3
$y^{10}P_{7/2}$	2.222	2.193	2.155±.0064	3
$y^{8}D_{7/2}$	1.809	1.793	1.79 ±.01	2
$y^{8}D_{5/2}$	2.057	2.042	2.025±.0047	5
$y^{8}D_{3/2}$	2.800	2.759	2.745±.01	1
$z^{6}D_{3/2}$	1.867	1.201	1.18 ±.02	1
$z^{6}D_{1/2}$	3.333	-0.491	-0.41 ±.02	1
$y^{8}F_{9/2}$	1.576	1.578	1.56 ±.02	1

Level	L-S	S-W	Obs.	No. of Obs.
$y^8F_{7/2}$	1.619	1.618	1.60 ±.02	1
$y^8F_{5/2}$	1.714	1.701	1.69 ±.01	1
$y^6P_{5/2}$	1.886	1.896	1.82 ±.02	1
$y^6P_{3/2}$	2.400	2.417	2.40 ±.02	1
$^4_{5/2}$	-----	-----	2.325±.0058	6

CHAPTER IV

ANALYSIS

4.1 The $4_{5/2}$ Level

A qualitative intensity rule for multiplet transitions gives the stronger lines as arising where orbital angular momentum changes in the same direction as total angular momentum. Of these, the strongest line arises from transitions involving the largest value of L and J. Transitions with $4_{5/2}$ which have been classified involve the levels listed in Table 4.1.

TABLE 4.1

Config$^{n.}$	Level	Wavelength	Intensity
6s5d	$a^6D^o_{5/2}$	5555.28	20
$5d^2$	$a^{10}P^o_{7/2}$	5545.01	250
6s5d	$b^8D^o_{5/2}$	5213.04	5
$5d^2$	$a^{10}F^o_{7/2}$	4140.450	100
$5d^2$	$a^{10}F^o_{5/2}$	4094.478	300
$5d^2$	$a^{10}F^o_{3/2}$	4063.59	200
6s5d	$a^8D^o_{7/2}$	3966.850	15
6s5d	$a^{10}D^o_{7/2}$	3524.196	1000
6s5d	$a^{10}D^o_{5/2}$	3491.954	2000

The observed g-value of the $4_{5/2}$ level is 2.325 and the energy level is listed as 28629.06 cm^{-1}. Table 4.2 lists the J = 5/2 even levels which are energetically close to this level

and which may be mixing with it.

TABLE 4.2

Level	Energy (cm^{-1})	L-S	S-W	Obs.	Mixing (S-W)
$z\,^{10}F_{5/2}$	26211.96	2.229	2.185	2.171	$80(^{10}F)12(^{8}D')$
$z\,^{8}P_{5/2}$	27297.77	2.286	2.373	2.536	$37(^{10}D)19(^{8}P_D')19(^{8}P_C)$
$z\,^{10}D_{5/2}$	29197.93	2.572	2.397	2.308	$49(^{10}D)38(^{8}P_C)$
$z\,^{8}D_{5/2}$	29965.81	2.057	2.097	2.043	$54(^{8}D')22(^{8}D)17(^{10}F)$
$y\,^{8}P_{5/2}$	32150.19	2.286	2.238	1.80	$34(^{8}P_D')23(^{8}P_C)13(^{8}P_C')$
$z\,^{8}F_{5/2}$	32260.16	1.715	1.781	2.173	$67(^{8}F)17(^{8}F')$
$z\,^{6}P_{5/2}$	32750.45	1.886	1.946	1.94	$79(^{6}P_C)12(^{8}P_C)$

The last column gives the percentage admixture of different levels through configuration interaction as predicted by Smith and Wybourne. The subscript C and D refer to the configurations $4f^7(^8S)6p6s$ and $4f^7(^8S)5d6p$ respectively, and the primes indicate terms with the same designation arising from the same configuration.

The $4_{5/2}$ level would seem to be a mixture of the following even levels: $^{10}D_{5/2}$ $^{8}P_{5/2}$ $^{10}F_{5/2}$. The $^{10}D_{5/2}$ character of this level is indicated by the strong intensities observed in transitions with the $^{10}D^o_{5/2\ 7/2}$ levels, the $^{8}P_{5/2}$ $^{10}F_{5/2}$ character by the moderate intensities with the $^{10}P^o_{7/2}$ $^{6}D^o_{5/2}$ and the $^{10}F^o_{3/2\ 5/2\ 7/2}$ levels respectively. The observed g-value of 2.325 would be a mixture of the g-values 2.572, 2.286, 2.229 belonging to the three levels concerned.

The most probable configuration giving rise to this $^4_{5/2}$ level would be $4f^7(^8S)5d6p$. This is indicated by the fact that the observed transitions are to the odd levels arising from $4f^7(^8S)5d6s$ and $4f^7(^8S)5d^2$ configurations, and would involve one electron jump only. However Russel (Ru 50) has refrained from assigning any of the P-terms to specific configurations because of the extensive "sharing" of the classical properties of the levels. Thus all that can probably be said is that the $^4_{5/2}$ term consists of a mixture of the levels $^{10}D_{5/2}$ $^8P_{5/2}$ and $^{10}F_{5/2}$ involving the $4f^7(^8S)5d6p$ configuration.

4.2 Discussion of Observed g-Values

The experimental results obtained for the Landé g-factors are in general quite close to those forecast by Smith and Wybourne. Disagreement is usually in the second decimal place, the theoretical correction from L-S coupling being mostly in the right direction but not large enough. Smith (Si 66) had this to say:

> It does not surprise me that disagreement with our calculated g_J values arises in the second decimal place. The calculations were based on a number of assumptions - use of sub-configurations etc. - and it is impossible to gauge the reliability of the results. By treating the Slater parameters as free variables we may have obtained a "forced" fit. It is well known that this approach does not take care of all possible types of "weak" configuration interactions (e.g. Wybourne: Phys. Rev. 137, A364, 1965). A fit to g_J values as well as to energy levels would provide a much more stringent solution. I believe that the "Racah"

> group in Jerusalem is working on the development of such a program. Unfortunately I no longer have the facilities for such sophisticated calculations.

Wybourne (Wy 66) for his part had this to remark:

> I would expect that relativistic effects would enter in the first or second decimal place in the g values but do not think that the discrepancies you have are simply due to ignoring relativistic effects. Rather I suspect some of the states are very sensitive to small changes in the eigenfunctions. The calculations that Geoffrey Smith and I did made use of the limited data that was available in the literature and could have been sustantially improved if there was more data available. Nevertheless we thought it worthwhile to publish these results so as to encourage experimentalists to refine the data and obtain additional data.

The g-values for one particular multiplet show a wide discrepancy between theory and experiment, the y^8P multiplet, as may be seen from Table 4.3. It would seem that this particular multiplet is mixing with other levels far more than predicted. Smith (Sm 66) has suggested that these levels may be mainly ^8F and that consequently some other levels would be biased towards ^8P. Following this line of thought, it has been found that indeed the ^8F and ^8P multiplets are mixing extensively together for those values of J which are common to both, but show practically no mixing otherwise. Column 7 shows the percentage mixing of levels as calculated from the observed g-values, and column 8 the corresponding calculated g-value. It will be noted that the $z^8F_{1/2\ 3/2}$ levels, with no corresponding levels in the ^8P multiplet, show practically pure L-S coupling.

TABLE 4.3

MIXING OF ENERGY LEVELS IN THE $4f^7 6p6s_C$ AND $4f^7 5d6p_D$

ELECTRON CONFIGURATIONS OF GD II

Energy	Level	L-S	S-W	Obs†	Mixing (S-W)¶	Mixing (Obs)	Calc. g
32150	$y^8P_{5/2}$	2.286	2.238	1.80(2)	$34(^8P'_D)23(^8P_C)13(^8P'_C)$	$80(^8F)20(^8P)$	1.825
32263	$y^8P_{7/2}$	1.937	1.933	1.743(2)	$37(^8P'_D)14(^8P_C)17(^8P'_C)$	$61(^8F)39(^8P)$	1.743
32304	$y^8P_{9/2}$	1.778	1.783	1.746(5)	$48(^8P'_D)25(^8P_C)$	$16(^8F)84(^8P)$	1.746
31977	$z^8F_{1/2}$	4.000	3.988	3.97(2)	$80(^8F)20(^8F')$	$100(^8F)$	4.000
32049	$z^8F_{3/2}$	2.000	2.007	2.01(1)	$78(^8F)19(^8F')$	$100(^8F)$	2.000
32260	$z^8F_{5/2}$	1.714	1.781	2.173(6)	$67(^8F)17(^8F')$	$80(^8P)20(^8F)$	2.173
32491	$z^8F_{7/2}$	1.619	1.653	1.791(7)	$63(^8F)16(^8F')$	$61(^8P)39(^8F)$	1.812
32685	$z^8F_{9/2}$	1.576	1.599	1.622(4)	$62(^8F)17(^8F')$	$16(^8P)84(^8F)$	1.608
27298	$z^8P_{5/2}$	2.286	2.373	2.536(3)	$37(^{10}D)19(^8P'_D)19(^8P_C)$	$87(^{10}D)13(^8P)$	2.534
29198	$z^{10}D_{5/2}$	2.572	2.397	2.308(7)	$49(^{10}D)38(^8P_C)$	$87(^8P)13(^{10}D)$	2.321
40092	$z^6D_{3/2}$	1.867	1.201	1.18(2)	$10(^6D)84(^6F)$		
40162	$z^6D_{1/2}$	3.333	-0.491	-0.41(2)	$96(^6F)$		

† numbers in brackets indicate error in last digit
¶ this column contains only contributions greater than 10%

Also included in Table 4.3 are the results of the calculations for mixing between the terms z^8P and $z^{10}D$. The g-values obtained for J=5/2 levels are in marked disagreement with those forecast by Smith and Wybourne. The percentage compositions calculated from the observed g-values appear in column 7. No entries are included for the levels J=7/2 and J=9/2 for these two terms, since in these cases the calculations of Smith and Wybourne do not seriously disagree with observation (Table 3.3, p. 49).

A particular effort was made to locate on the spectrograms patterns involving levels for which the S-W corrections to the L-S values were unusually large. Such patterns were found involving the $z^6D_{3/2}$ and $z^6D_{1/2}$ levels. The corresponding g-values are also included in the same table. Although these results are much less accurate due to the faintness of the patterns, nevertheless they indicate that the S-W calculations are not seriously in error for these levels. It is interesting to see that their calculations are so successful in this extreme case.

A detailed analysis of other discrepancies between theory and experiment was not attempted, as generally the mixing occurs between more than two levels and a computer programme would be required. Such "sophisticated calculations" are more properly the domain of the theoretical physicist working with data provided by the experimentalist.

CHAPTER V

SUMMARY

It may be noted here that the present investigation of Zeeman effect in singly ionized gadolinium has been attempted twice, once using a grating blazed to first and second orders in conjunction with an assortment of filters and photographic plates, and a second time using a high-blaze grating with order sorter. This grating was not employed originally because it was not immediately available.

The results obtained using the grating blazed for high orders are more accurate than earlier results by a factor of ten. In fact, the mean error for the g-values obtained is less than 0.5%, with 25 of the better results having a mean error of 0.12%. This increase in accuracy would seem to be one major accomplishment of this work.

An attempt has been made to interpret these results in the light of configuration interaction for a few special cases. A more thorough analysis was felt to be beyond the scope of this work. The calculations of Smith and Wybourne themselves have been found to be an improvement over the pure L-S coupling scheme neglecting term mixing, the correction from L-S coupling being in the right sense for 80% of the levels investigated. On the other hand

agreement within experimental error was found for only 18% of the levels. It was mentioned at the beginning of this thesis that the incentive to investigate the Zeeman effect in Gd II was provided by the theorists' appeal for experimental data. It is to be hoped that the data here presented will in turn encourage the theorists to improve their calculations and hence man's understanding of the atom.

APPENDIX

A-1 Terminology

The specialized terminology used in spectroscopy may require a few words of explanation.

The word "state" is used very generally and may mean term, level or component depending on the context. An electronic configuration is a statement of the number of occupied wave functions in each group having definite (nl) quantum numbers. For example, the electronic configuration for Gd II is the following: $1s^2 2s^2 2p^6 3s^2 3p^6 3d^{10} 4s^2 4p^6 4d^{10} 4f^7 5s^2 5p^6 5d6s$. The energy states of an electron may be classified into terms and levels; in what is called Russel-Saunders (or L-S) Coupling, a level comprises all those states which in the absence of an external magnetic field have the same energy, depending on L, S, and J, e.g. the levels $^3P_2$ or $^3P_1$. The variation in energy between levels of the same L and S but different J depends on spin-orbit interaction and is frequently referred to as fine-structure. If spin-orbit interaction is neglected, we obtain a set of terms depending on L, S only, e.g. the terms ^3P or ^1P.

Thus a term is a set of states of the same energy in the absence of an external magnetic field and of spin-orbit interaction;

a term is split into levels by spin-orbit interaction (fine structure), and a level is further split into Zeeman components by an external magnetic field, or into Stark components by an external electric field, or into hyperfine structure components by interaction with the nuclear magnetic moment.

A-2 Theory of the Zeeman Effect

The anomalous Zeeman effect was first explained successfully by what later became known as the Vector Model of the atom. The advent of the Quantum Theory confirmed and refined the results obtained. The vector model gives a satisfactory description of many spectroscopic observations; it is simple and easily visualized, and hence is a useful concept. Just as physical optics has complemented and improved upon geometrical optics, so the Quantum Theory has refined the results obtained by the vector model.

According to the vector model, the orbital motion of the electron produces a magnetic moment

$$\mu_\ell = M_B \ell^*$$

and the spin of the electron a magnetic moment

$$\mu_s = 2M_B s^*$$

where $M_B = eh/4\pi mc$ is the Bohr magneton, $\ell^* = \sqrt{\ell(\ell + 1)}$ is the orbital angular momentum q.n. and $s^* = \sqrt{s(s + 1)}$ is the spin angular momentum q.n.

Although the resultant of μ_ℓ and μ_s is not parallel to $j^*=\sqrt{j(j+1)}$, the total angular momentum q.n., only its component parallel to j^* contributes to the magnetic moment of the atom, the perpendicular component averaging out to zero.

The vector sum of μ_ℓ and μ_s parallel to j^* yields

$$\mu_j = M_B j^* g$$

where g, the Landé splitting factor, is given by

$$g = 1 + \frac{j(j+1) + s(s+1) - \ell(\ell+1)}{2j(j+1)}$$

The change in the motion of an electron about a nucleus produced by the introduction of a magnetic field is a precession of the orbit about this field with uniform angular velocity. The corresponding change in the energy of the electron due to its precession about the field H (Larmor precession) is given by

$$\begin{aligned}\Delta E &= H\mu_j \cos(j^*H) \\ &= HM_B j^* g \cos(j^*H) \\ &= HM_B g m_j\end{aligned}$$

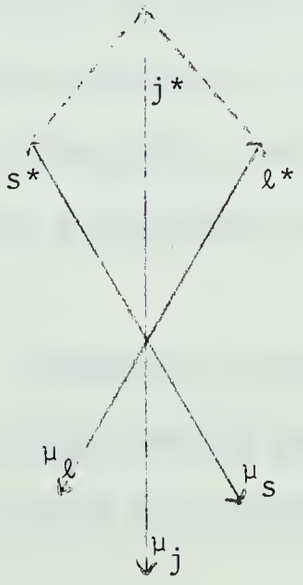

where m_j, the magnetic q.n., is the projection of j on H and takes on values j, j - 1, ... -j. The energy change in wave numbers is then given by

$$\Delta\nu = \frac{eH}{4\pi mc^2} m_j g = Lgm_j$$

where L is the Lorentz unit.

The Zeeman splitting is thus directly proportional to g, the Landé splitting factor, L being a constant for a given field. The selection rules for light emitted perpendicularly to the field are

$\Delta m = \pm 1$; plane polarized: perpendicular to H (σ components)

$\Delta m = 0$; plane polarized: parallel to H (π components)

The beauty and power of Zeeman analysis is that, for a well resolved Zeeman pattern, a precise knowledge may be gained of the J-values of the levels involved in the transition and the relative magnitude of one g-value with respect to the other. The method for obtaining this knowledge is described in the following section.

A-3 Method of Determining g-Values from Observed Patterns

Tables giving the displacement and the intensity of the components can be derived from theoretical considerations. The spectrogram measurements are put automatically on "punch cards" and these are fed to a computer. The computer makes a comparison of the experimental pattern with that calculated theoretically, yielding a knowledge of the type of transition.

However it is preferable in general to calculate the J-value and g-value from the pattern itself. The following procedure has been adopted in the present work.

The displacement of an energy level due to the action of the field can be expressed in wave numbers per Lorentz unit

$$m_J g = \Delta\nu L^{-1}$$

Allowed transitions between these Zeeman states lead to a set of equations in two unknowns, the two g-values belonging to the states involved. Taking e as the average spacing of the π components and 2f as the distance between two σ components, these equations take the form

$$g_x - g_y = \pm e$$

$$m_x g_x - m_y g_y = \pm f$$

where g_x g_y are the two g-values and m_x m_y are the magnetic q.n.

The solution of this set can be found by computer (Va 56). This has not been done in the present work mainly in order to gain experience with the type of patterns met. Furthermore, it was possible by calculating manually to check each pattern while its calculation was being made, and hence to allow for the pecularities of each individual pattern. For example, one pattern might be over-exposed, another partially masked and so on. It was not felt that these judgments could be made as accurately by computor.

The resulting equations take on special form depending on the three main types of patterns given in Appendix 4. Once a solution has been obtained, the g-values are substituted in the set

of equations and the calculated spacings e and f are compared with the observed values. If the fit is unsatisfactory, a different choice of components can be made until a satisfactory fit is obtained.

A-4 Possible Types of Zeeman Patterns

1. Symmetrical patterns: $J_x = J_y$

   Taking $g_x > g_y$, and choosing the strongest σ component (this may not necessarily be the best component to choose)

   a) J half-integral:

$$g_y - g_x = e$$

$$g_x + g_y = 2f$$

   b) J integral

$$g_y - g_x = e$$

$$g_x = f_1,\ g_y = f_2$$

   ($2f_1$ $2f_2$ are the distances between the two pairs of strongest lines)

2. Shade-In Patterns: $J_x > J_y$

   Then $g_x > g_y$. Choosing again the strongest σ component:

$$g_x - g_y = e$$

$$(J_y + 1)g_x - J_y g_y = f$$

3. Shade-Out Patterns: $J_x > J_y$

   Then $g_x < g_y$. For the strongest σ component:

$$g_y - g_x = e$$

$$(J_y + 1)g_x - J_y g_y = f$$

FIGURE A-1

Symmetrical Pattern: $J_x = J_y$, $g_x > g_y$

a) J half-integral, e.g. $^8F_{5/2}$ -- $^8G_{5/2}$, $J_x = 5/2$, $J_y = 5/2$

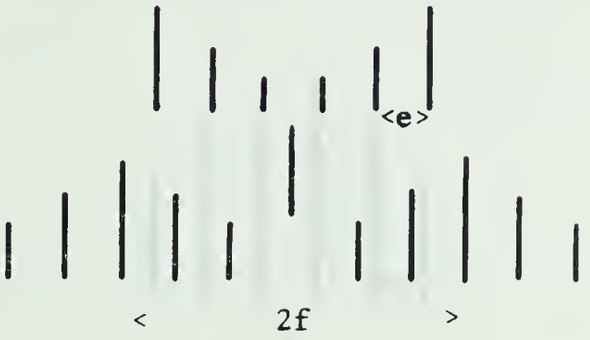

b) J integral, e.g. $^7F_3$ -- $^7G_3$, $J_x = 3$, $J_y = 3$

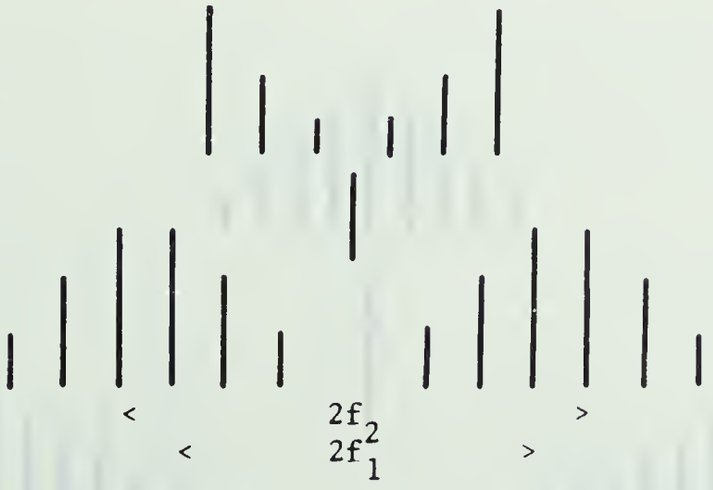

FIGURE A-2

Shade-In Pattern: $J_x > J_y$, $g_x > g_y$

a) J half-integral, e.g. $^8F_{7/2}$ -- $^8G_{5/2}$, $J_x = 7/2$, $J_y = 5/2$

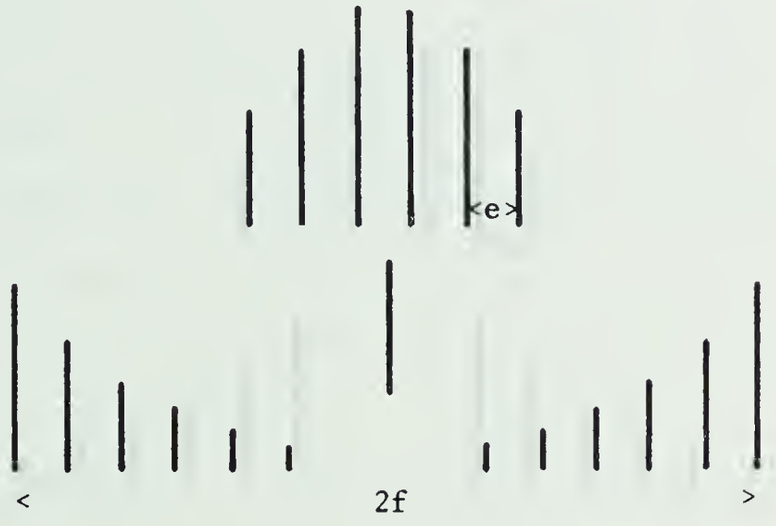

b) J integral, e.g. $^7F_5$ -- $^7G_4$, J_x 5, J_y 4

FIGURE A-3

Shade-Out Pattern: $J_x > J_y$, $g_x < g_y$

a) J half-integral, e.g. $^8G_{7/2}$ -- $^8F_{5/2}$, $J_x = 7/2$, $J_y = 5/2$

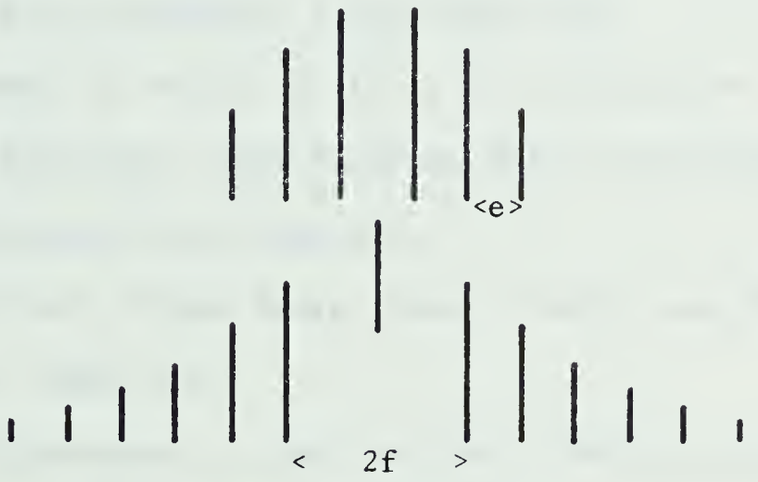

b) J integral, e.g. $^7G_5$ -- $^7F_4$, $J_x = 5$, $J_y = 4$

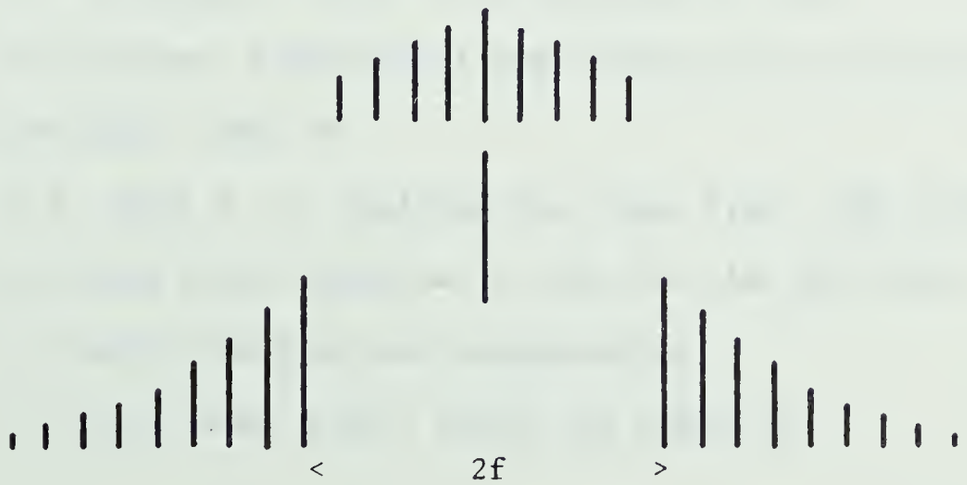

LIST OF REFERENCES

Ga 59 A. Gatterer & J. Junkes, Atlas der Restlinien, Vol. II, Spektren der Seltenen Erden (Specola Vaticana Laboratorio Astrofisico, Città del Vaticano, 1959)

Ka 25 H. Kayser, Tabellen der Schwingungszahlen (S. Hirzel, Leipzig, 1925)

Ki 43 A.S. King, Astrophys. J. 97 (1943) 323

La 21 A. Landé, Z. Physik, 5 (1921) 23; 7 (1921) 399

Mi 06 A.A. Michelson, Light Waves and Their Uses (University of Chicago Press, 1906) 107

Mo 58 C.E. Moore, Atomic Energy Levels, (Natl. Bur. Standards Circ., 1958) 467

Pi 67 E.H. Pinnington, J. Opt. Soc. Am. (1967) 57. 271

Pr 98 T. Preston, Phil. Mag. 45 (1898) 325

Re 63 J. Reader, L.C. Maquet & S.P. Davis, Applied Optics (1963) 963

Ru 50 H. N. Russel, J. Opt. Soc. Am., 40 (1950) 550

Sa 63 R.A. Sawyer, Experimental Spectroscopy (Dover Publications, New York, 1963) 79

Sm 61 K.F. Smith & I.J. Spalding, Roy. Soc. Proc., 265 (1961) 133

Sm 65 G. Smith & B.G. Wybourne, J. Opt. Soc. Am. 55 (1965) 1278

Sm 66 G. Smith (1966) private communication

St 13 J. Stark, Akad. Wiss., Berlin, 40 (1913) 932

To 51 F.S. Tomkins & M. Fred, J. Opt. Soc. Am. 41 (1951) 641

To 55 J. Topping, Errors of Observation (Inst. Physics, 47 Belgrave Sq., London, 1955) 89

Uh 25 G.E. Uhlenbeck & S. Goudsmit, Naturwissenshaften, 13 (1925) 953; Nature, 117 (1926) 264

Va 56 K.L. Vander Sluis, J. Opt. Soc. Am. 46 (1956) 605

Wo 63 E.F. Worden, R.C. Gutmacher & J.G. Conway, Applied Optics, 2 (1963) 707

Wy 65 B.G. Wybourne, Spectroscopic Properties of Rare Earths (Interscience Publishers, Wiley & Sons, New York, 1965) 102

Wy 66 B.G. Wybourne (1966) private communication

Ze 97 P. Zeeman, Phil. Mag. (5) 43 (1897) 226